2018 TIGeR CONFERENCE

Coupling between Metamorphism and Deformation

Post-Conference Field Trip Guide

The Leeuwin Complex Western Australia

15-17 September 2018

THE INSTITUTE FOR GEOSCIENCE RESEARCH (TIGeR)

Make tomorrow better.

Curtin University

2018 TIGeR CONFERENCE

Coupling between Metamorphism and Deformation

Curtin University, Perth, Western Australia

12-14 September 2018

Post-conference Field Trip Guide: The Leeuwin Complex, Western Australia

Saturday 15th to Monday 17th September, 2018

Nicholas E. Timms[1]

email n.timms@curtin.edu.au

With contributions from Ian Fitzsimons[1], Paul Wilkes[2], Tim Johnson[1], David Pearce[1,3], Chris Tucker[1], Sarah Arnoldi[1], Hugo Olierook[1], and Steven Reddy[1].

[1] Curtin University, Perth, GPO Box U1987, Western Australia

[2] CSIRO, Perth, Western Australia

[3] CMW Geosciences, Australia

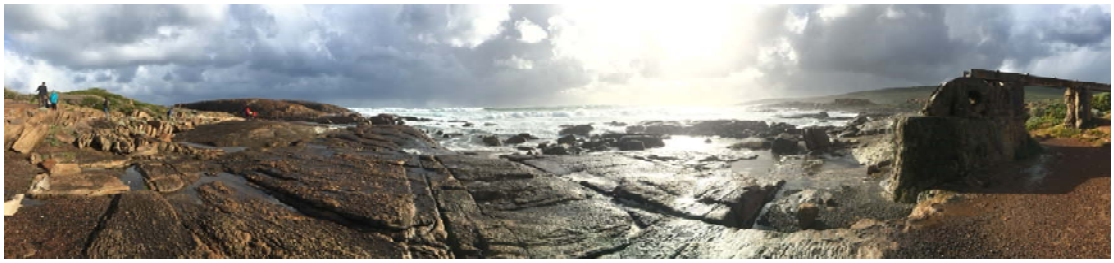

Cape Leeuwin waterwheel (image = Nick Timms)

Table of Contents

Welcome to southwest Western Australia

The objective of this field trip is to discuss the geological evolution of the southwestern-most corner of Australia. On this trip, we will focus on the coastal outcrops of the Mesoproterozoic to Cambrian crystalline rocks of the Leeuwin Complex in the southwestern-most corner of Australia. We will explore the role of this enigmatic puzzle piece in the assembly and breakup of Gondwana, showcasing new interpretations based on recent geophysical imagery, geochronology, and field data. We may also visit outcropping lava flows of the Bunbury Basalt within the Perth Basin, which represent the first vestiges of continental breakup. Several previous field guides have focussed on this region (Myers, 1994; Nelson, 1995; Wilde and Nelson, 2001; Janssen et al., 2003; Freeman and Donaldson, 2006, 2008; Timms, 2017, 2018). The aim of this field guide is to provide updates of some key data and recent findings, contemporary views, and potential future research directions. It showcases new interpretations based on geophysical imagery, geochronology and mapping, and explores the assembly and breakup of eastern Gondwana. A thorough review on the historical development of ideas is not offered to keep this document succinct. Readers are directed elsewhere for detailed reviews, e.g., Myers (1990c), Iasky (1993), Harris (1994b), Wilde and Murphy (1990), Fitzsimons (2003), and Janssen et al. (2003). Research in the area is ongoing, and a variety of new data are currently being acquired. Consequently, some ideas summarized here may be subject to change, even since I wrote this field trip guide!

The Leeuwin Complex is situated in the heart of the Margaret River region, famous for fine wine, world-class surfing, whale watching, and beautiful Karri forests. I hope that you enjoy the trip! *Nick Timms*

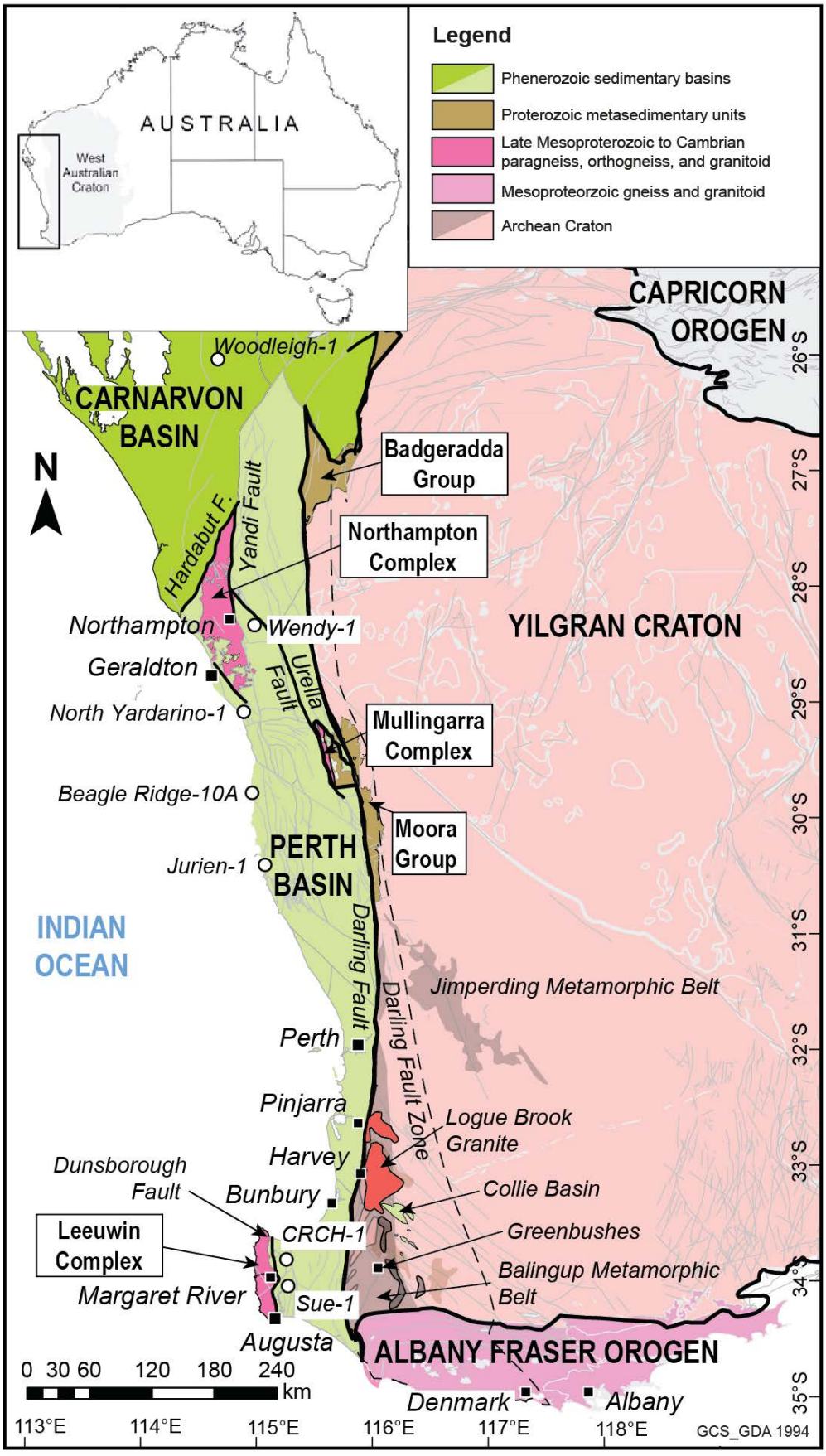

Figure 1. *Simplified map of the bedrock geology of southwest Western Australia showing major tectonic subdivisions. After Wilde and Nelson (2001), Janssen et al. (2003) and Markwitz et al. (2017). The Pinjarra Orogen comprises components labeled by white boxes.*

Evolution of the southwestern margin of Western Australia

The region along the western margin of the Archean Yilgarn Craton - what now forms the western seaboard of Western Australia - has undergone numerous major geological events, including multiple episodes of continental amalgamation and break-up (Collins, 2003). However, there are aspects of the geological history that are still not well understood. This in part is due to the limited exposures: The Yilgarn Craton is poorly-exposed, adjacent crystalline rocks outcrop only in three widely-spaced inliers (Northampton, Mullingarra and Leeuwin Complexes) (Myers, 1990c), and the onshore Perth Basin is mostly veneered by Quaternary to recent deposits (Playford et al., 1976) (Figs 1 and 2). Furthermore, the rifted geological counterparts to southwest Western Australia are buried under ice sheets in Antarctica, subducted beneath Tibet, or covered by alluvial and fluvial systems in India. Consequently, the rocks of southwestern Western Australia continue to attract attention because they represent important puzzle pieces due to the unique position that they occupy, the protracted geological history that they record, and their role in paleo-continent reconstructions (Norvick et al., 2001; Fitzsimons, 2003; Veevers et al., 2007; Boger, 2011; Williams et al., 2011; White et al., 2013; Aitken et al., 2016; Morrissey et al., 2017; Tucker et al., 2017).

The southwestern Yilgarn Craton

The South West Terrane of the Yilgarn Craton has a rich history and has been subdivided into three metamorphic belts, from southwest to northeast these are the Balingup, Chittering and Jimperding Metamorphic Belts (Fig. 1) (Wilde, 1999; Wilde and Nelson, 2001). Metasedimentary rocks and orthogneiss in the Balingup zone have undergone amphibolite facies metamorphism, the age of which is poorly constrained, but is considered to be > ca. 2838 Ma (Wilde and Nelson, 2001). These rocks are intruded by granitoids of the 2612 ± 5 Ma Logue Brook Granite, 2647 to 2613 Ma Darling Range Batholith and the ca. 2828 to 2740 Ma Gibraltar Quartz Monzonite (Compston et al., 1986; Nemchin and Pidgeon, 1999; Wilde, 1999; Wilde and Nelson, 2001) (Fig. 3). Intrusion of syntectonic pegmatites occurred at ca. 2577-2527 Ma, with the shear zone-hosted Greenbushes Pegmatite, south of Balingup, forming the world's most significant lithium and tantalum deposits (Partington et al., 1995; Wilde and Nelson, 2001; Freeman and Donaldson, 2008).

The southwestern Yilgarn Craton has been intruded by several sets of mafic dyke swarms, the earliest being the 2418 ± 3 Ma E-W trending Widgemooltha Dyke Swarm (Nemchin and Pidgeon, 1998). Four other intersecting swarms are visible on the Yilgarn Craton adjacent to the western Albany-Fraser Orogen. NW-SE, E-W and ENE-WSW sets that are attributed to the Boyagin, Gnowangerup, and Fraser dyke swarms, respectively, plus a WNW-ESE trending set that is unassigned (Myers, 1990a; Harris and Li, 1995). These dykes yield ages of ca.1218 Ma to ca. 1202 Ma (Evans, 1999; Qiu et al., 1999; Wingate et al., 2000; Pidgeon and Nemchin, 2001; Pidgeon and Cook, 2003; Rasmussen and Fletcher, 2004; Wingate and Kirkland, 2011; Pisarevsky et al., 2014), and are contemporaneous with events of Stage II of the Albany-Fraser Orogen to the south (Spaggiari et al., 2014).

The Darling Fault Zone

A westward increase in abundance of ~N-S trending, ribbon-like mylonite and ultramylonite zones indicates a general increase in strain towards the Darling fault, which bounds the western edge of the Yilgarn Craton (Wilde, 1999; Wilde and Nelson, 2001) (Fig. 1). Along the soutwestern margin of the Yilgarn Craton, high strain zones up to 10 km wide are interpreted to be part of a crustal-scale sinistral ductile shear zone, known as the Darling Fault Zone, that was periodically reactivated during the Proterozoic, and along which the brittle(?) Darling Fault nucleated with normal sense during the Phanerozoic (Dentith et al., 1993; Harris, 1994a; Beeson et al., 1995; Wilde and Nelson, 2001).

The southern margin of Yilgarn Craton is bound by the Proterozoic (ca. 1850-1100 Ma) Albany-Fraser Orogen (Fig. 1). No rocks of Albany-Fraser affinity have been demonstrated to occur onshore west of the Darling Fault. The entire Albany-Fraser Orogen is deflected southward in an apparent sinistral sense by the Precambrian Darling Fault Zone (Fig. 1). Even though this relationship is clearly visible on aeromagnetic images, exposed N-S trending Albany-Fraser rocks is limited to very weathered outcrops Windy Harbour. Nevertheless, protolith and metamorphic age constraints from rocks of the Albany-Fraser Orogen to the east mean that sinistral ductile shearing associated with the Darling Fault Zone must be younger than ca. 1100 Ma. Recrystallization and resetting of $^{40}Ar/^{39}Ar$ ages of micas from Archean rocks on the western margin of the Yilgarn Craton in the vicinity of Perth preserve ages down to ca. 620 Ma adjacent to the Darling Fault to ca. 1320 Ma up to 40 km to the east (Lu et al., 2015) (Fig. 3). The southwest Yilgarn and Albany-Fraser Orogen have been susceptible to resetting of the Rb-Sr system in biotite to as young as ca. 405 Ma in the vicinity of the town of Harvey (Libby and de Laeter, 1998) (Fig. 3).

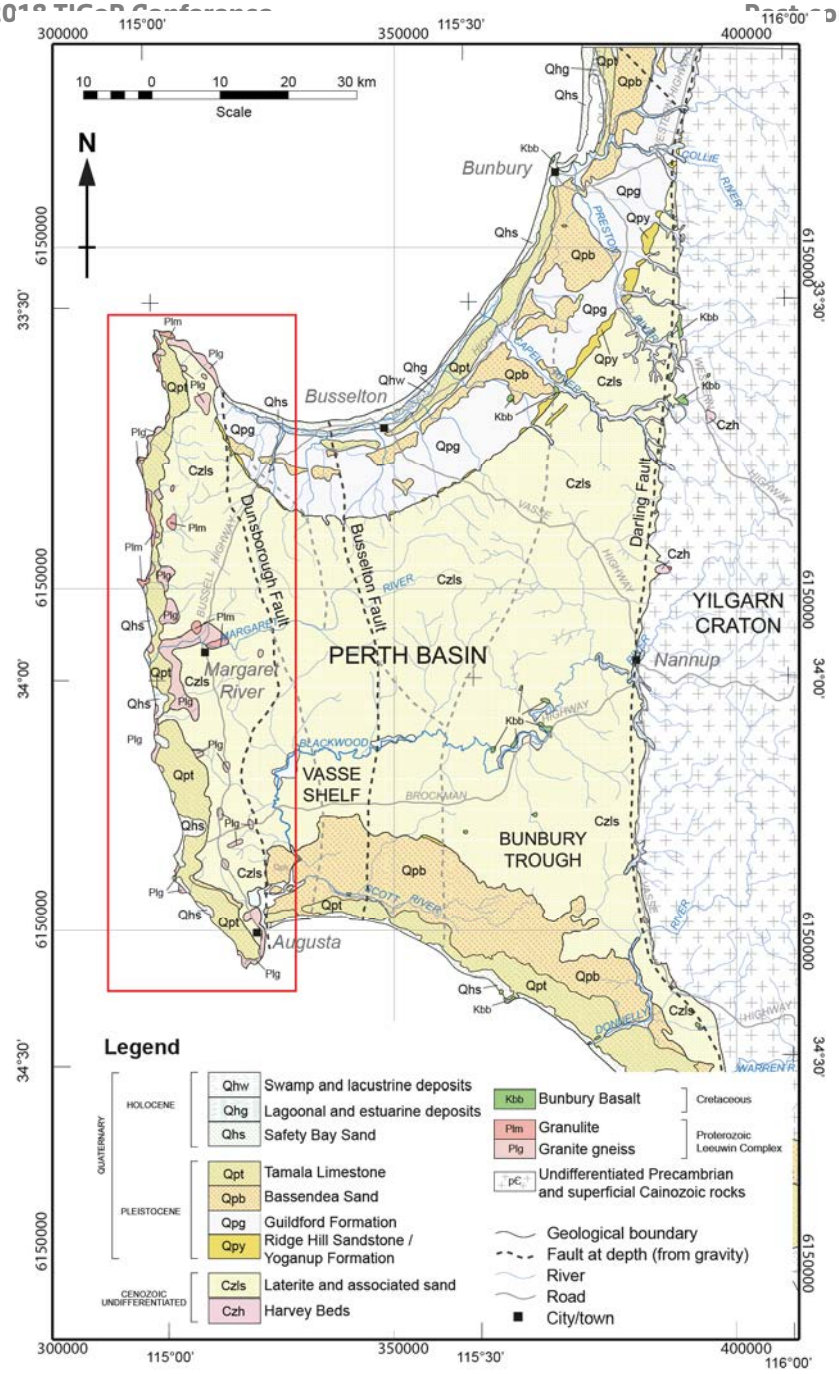

***Figure 2**. Geological map of southwestern Western Australia showing the location of the Leeuwin Complex. After Playford et al. (1976).*

Pinjarra Orogen

Basement rocks to the west of the Darling Fault from the southern coast of Australia over 1500 km north are exclusively Proterozoic to Cambrian in origin, were once referred to as the Darling Mobile Belt (Harris, 1994a; Wilde and Nelson, 2001), and are more generally known as the Pinjarra Orogen (Myers, 1990c). Later, the Pinjarra Orogen was defined to refer specifically to accretion of a belt of terranes to the western margin of the Yilgarn Craton and reworking of the Yilgarn margin during Neoproterozoic to Cambrian times (Myers et al., 1996; Fitzsimons, 2003; Janssen et al., 2003) (Fig. 1). These authors make the distinction that the terranes that were accreted have an older history, which they interpret to be unrelated to accretion event associated with the Pinjarra Orogen, *sensu stricto*. Events ca. 1100-1000 Ma have been referred to as the Proto-Pinjarra Orogen (Myers et al., 1996). Lu et al. (2015) subdivided the Pinjarra Orogen into two orogenic events: Stage I (Pinjarra Orogeny) between ca. 1000-1270 Ma; and Stage II (Leeuwin Orogeny) between ca. 500810 Ma. However, the exact nature of tectonic activity during this time will be a topic of discussion during the trip.

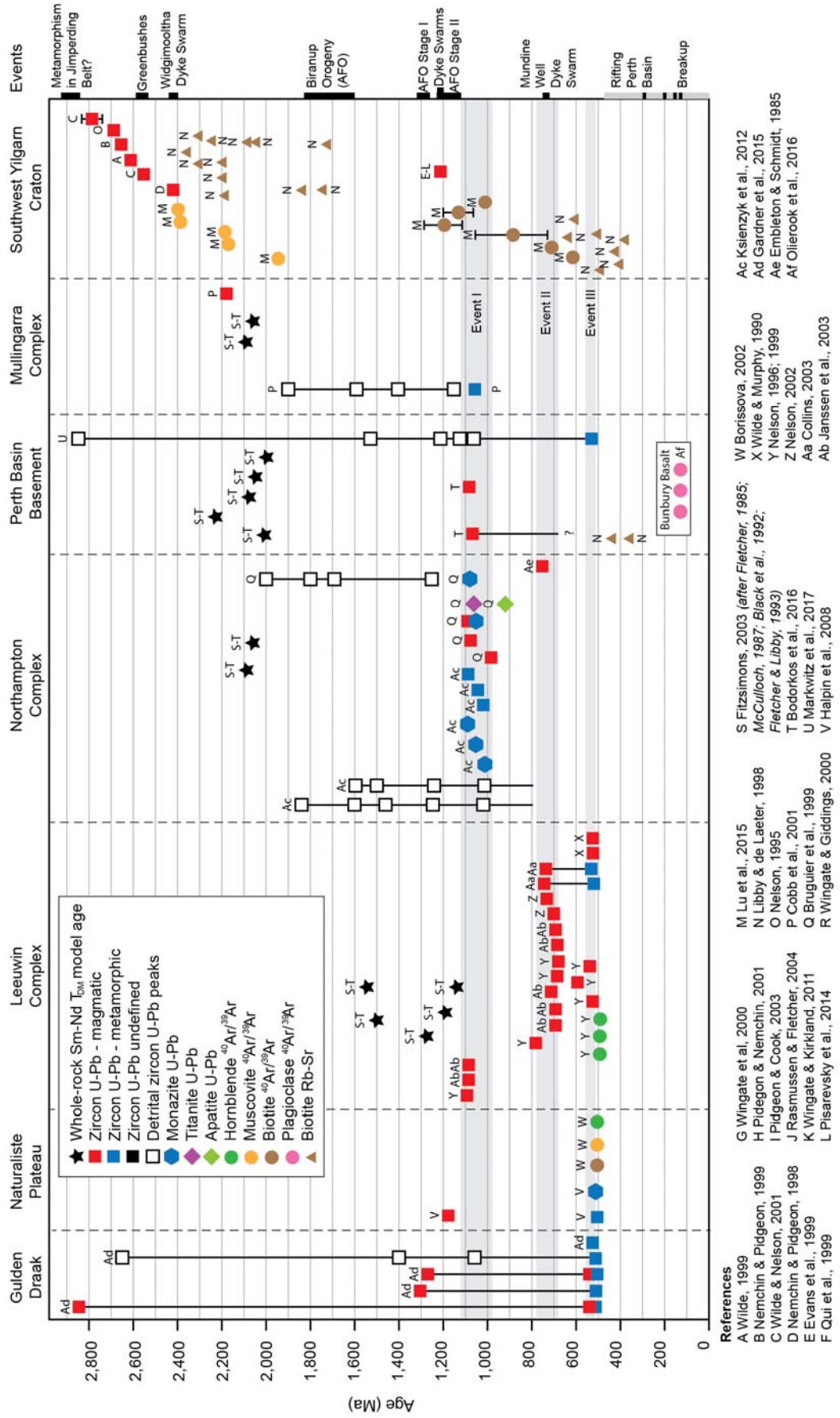

Figure 3. *Compilation of geochronological data for the southwest Western Australia.*

Outcrops of the Pinjarra Orogen are restricted to three fault-bound basement inliers – referred to as the Northampton, Mullingarra, and Leeuwin Complexes, and low-grade metasedimentary rocks of inferred Proterozoic age that unconformably overlie the Yilgarn Craton and Mullingarra Complex to the north of Perth (Myers, 1990c) (Fig. 1). Elsewhere, the Pinjarra Orogen is covered by sedimentary rocks of the Perth Basin, and only a small number of petroleum exploration wells have intersected basement rocks (Fletcher et al., 1985; Fletcher and Libby, 1993; Bodorkos et al., 2016; Markwitz et al., 2017) (Figs 1 and 3).

Northampton and Mullingarra Complexes

Two of the three inliers of the Pinjarra Orogen share similar geological characteristics. The Northampton and Mullingarra Complexes are located near the towns of Geraldton and Three Springs, respectively, and have been described in detail by Myers (1990c) (also see Janssen et al. (2003) for a summary). The Northampton and Mullingarra Complexes predominantly comprise psammititic paragneiss, metapelite, quartzite and mafic gneiss. The detrital provenance of these metasedimentary units is generally upon as the Albany-Fraser Orogen (Fitzsimons, 2003; Ksienzyk et al., 2012). SHRMIP U-Pb detrital zircon age spectra show populations at 1900-1600 Ma and 1400-1150 Ma in both complexes, with a maximum depositional age of 1113 ± 26 Ma (Cobb et al., 2001; Ksienzyk et al., 2012) (Fig. 3). These ages are consistent with source rocks of either the Albany-Fraser or Capricorn Orogens (Fitzsimons, 2003; Spaggiari et al., 2011; Ksienzyk et al., 2012; Spaggiari et al., 2014). Metamorphism reached granulite facies at 1079 ± 3 in the Northampton Complex and peak amphibolite facies conditions at 1079 ± 32 Ma in the Mullingarra Complex, shown by SHRIMP U-Pb zircon analyses (Bruguier et al., 1999; Cobb et al., 2001).

The Mullingarra Complex hosts an unmetamorphosed monzogranite with a zircon population of 2181 ± 10 Ma (Cobb et al., 2001). Felsic magmatism in the Northampton Complex is represented by a 1068 ± 13 Ma granite pluton and pegmatite dyke emplacement at 989 ± 2 Ma (Bruguier et al., 1999) (Fig. 1). A N-NE trending mafic dyke swarm intruded the Northampton Complex at ca. 750 Ma (Embleton and Schmidt, 2007), and has been correlated with the Mundine Well dyke swarm in the Pilbarra Craton (Wingate and Giddings, 2000), but could possibly be associated with the similar-trending Muggamurra dyke swarm on the Yilgarn Craton (Janssen et al., 2003). No mafic dykes have been identified in the Mullingarra Complex.

The Leeuwin Complex

The Leeuwin Complex, which is a focus of this field trip, forms the crystalline basement of the Cape Leeuwin to Cape Naturaliste in the far southwest of Western Australia. Its onshore expression is approximately 20 km wide, and is bound to the east by the Dunsborough Fault, a normal fault that juxtaposes the Leeuwin Complex with the Vasse Shelf of the Perth Basin. The Leeuwin Complex continues offshore to the north, west and south, where it is obscured and draped by sediments (Fig. 2).

Outcrops of the Leeuwin Complex are generally limited to coastal headlands, with small patchy, isolated outcrops inland. Elsewhere onshore, the Leeuwin Complex is veneered by Cenozoic to recent sediments (Playford et al., 1976) (Fig. 2). The rocky headlands of the Leeuwin Complex and intervening beaches pick up swell from the Southern and Indian Oceans, and the region is renown for hosting world surf tournaments, such as the 'Margaret River Pro'. Inland, remnant patches of magnificent Karri forests endure among predominantly agricultural land use. Well-drained soils and the local climate have seen the establishment of this region, known as the Margaret River Region, for producing world-class wines. A combination of fine wine, pristine beaches warmed by the Leeuwin Current, good fishing, and excellent surf breaks are largely responsible for the popularity of the Cape to Cape region with tourists.

Eolianites of the Pleistocene Tamala Limestone are prevalent along coastal areas, reaching thicknesses of ca. 330 m in places and commonly deposited unconformably on the gneisses of the Leeuwin Complex (Playford et al., 1976). Hundreds of caves have been dissolved out of these units, and a handful of them are open to the public as show caves. Some of the caves have exploited the unconformity, providing an additional opportunity to access the Leeuwin Complex beneath.

The Leeuwin Complex mainly comprises of interleaved orthogneiss of felsic, intermediate and mafic composition, which is dissimilar to the Northampton and Mullingarra Complexes to the north. Many different lithological classification schemes based on different criteria have been developed over time, which can serve to confuse when comparing studies (Janssen et al., 2003). The relatively simple grouping into units of the mafic-dominated Cowaramup Gneiss and deformed granitoid Hamelin Granite by Myers (1994) was adopted by Collins (2003). More complex classification schemes were developed based on mineralogical criteria, resulting in six 'types' of gneiss (Wilde and Murphy, 1990; Murphy, 1992). In places, igneous protoliths can be inferred confidently from the preservation of primary textures and mineralogy (Myers, 1990b; Collins, 2003). However, the effects of deformation and metamorphism can be variable, interleaving can occur on different scales and migmatitic textures are common, which can make field mapping based on protolith types difficult. Gneisses of all compositions preserving variable proportions and geometries of leucosomes along strike and across strike. Granitoid pegmatites can

occur as planar dykes on the order of a few centimetres to tens of centimetres wide that cross cut most structures, or as nebulous blobs, some instances with ambiguous relationships to smaller-scale leucosomes. Conspicuous sharply-bound, black mafic bands generally much less than a metre in thickness are occasionally found interspersed with other gneisses, interpreted as the metamorphosed and deformed remnants of mafic dykes (Myers, 1990b; Wilde and Murphy, 1990; Simons, 2001; Collins, 2003).

Until recently, the deformation history of the Leeuwin Complex has been developed from detailed structural mapping of disjointed coastal outcrops (Myers, 1990b; Murphy, 1992; Collins, 2003; Harris, 2003; Janssen et al., 2003). A sequence of five deformation events (D_1 to D_5) in the northern Leeuwin Complex and four (D_1 to D_4) in the southern Leeuwin Complex has been suggested (Janssen et al., 2003). Structures assigned to these events are outlined below:

D_1 is taken to be the prominent gneissic foliation (S_1) and parallel lithological layering across the Leeuwin Complex. However, it is acknowledged that D_1 might not represent an initial deformation stage given that this foliation is axial planar to centimetre- to metre-scale, often rootless isoclinal fold (F_1) hinges. Leucosomes can be strongly parallel or weakly aligned with S_1. Asymmetric kinematic indicators in S_1 are typically either absent or have inconsistent shear senses.

D_2 is represented by north-trending, typically km-wavelength folds (F_2) that deform the D_1 foliation. These folds plunge gently to moderately northward in the northern Leeuwin Complex, and are tight with a steep northerly plunge in the southern Leeuwin Complex. An L_1^2 intersection lineation can be observed in the northern Leeuwin Complex.

D_3 is interpreted to be a late folding event (F_3) that does not result in new foliations or lineations. An ENE-trending F_3 fold has been inferred to explain a girdle distribution of F_2 fold hinges at Cape Naturaliste (Collins, 2003). In the southern Leeuwin Complex, D_3 is manifest as gentle folds with ~10 km wavelengths (Janssen et al., 2003), and open folding of S_1 in the northern Leeuwin Complex is attributed to D_4.

Brittle faulting of various scales and orientations has been allocated to D_4 in the southern Leeuwin Complex and D_5 in the northern Leeuwin Complex in the scheme of (Janssen et al., 2003). More recently, detailed field mapping has been combined with interpretation from aeromagnetic imagery to resolve the architecture of the Leeuwin Complex and develop a framework for its structural components (Pearce, 2014; Tucker, 2014). This will be discussed in detail below and during the trip.

The Leeuwin Complex was metamorphosed to upper-amphibolite to granulite facies conditions. Thermobarometric estimates for peak metamorphism include 6.85-7.6 kbar and 784-800 °C (Stoltze, 2000) and 5 kbar and 650-750 °C (Murphy, 1992) in the northern Leeuwin Complex. It has been proposed that the southern Leeuwin Complex did not reach granulite facies conditions (Wilde and Murphy, 1990), whereas the prevalence of amphibolite facies assemblages could simply reflect widespread retrogression of granulites (Myers, 1994).

The timing of events in the Leeuwin Complex has been constrained by SHRIMP U-Pb zircon, hornblende $^{40}Ar/^{39}Ar$ geochronology, and whole-rock Sm-Nd analysis (Fletcher et al., 1985; Wilde and Murphy, 1990; Fletcher and Libby, 1993; Nelson, 1996, 1999; Nelson, 2002; Collins, 2003; Fitzsimons, 2003; Janssen et al., 2003) (Figs 3 and 4a). The meaning of the data is still a matter of debate, and the subject of ongoing research (Arnoldi, 2017; Arnoldi et al., 2017). The earliest U-Pb zircon ages are recorded from garnet-bearing gneisses in the central Leeuwin Complex, and are ca. 1090 Ma, interpreted as magmatic crystallisation ages of the protoliths (Nelson, 1999; Janssen, 2001; Janssen et al., 2003). A younger group of U-Pb zircon analyses from rocks elsewhere define a spread of ages between ca. 780 and ca. 680 Ma (Nelson, 1996, 1999; Nelson, 2002; Collins, 2003). The final episode recorded by U-Pb zircon system is ca. 540-520 Ma (Wilde and Murphy, 1990; Collins, 2003). Lack of textural context for analyses in early studies (Nelson, 1996, 1999; Nelson, 2002) make the exact cause of the spread of ages difficult to interpret: potentially representing long-lived / repetitive igneous activity, metamorphic overgrowth or disturbance events, or some combination of these. Nevertheless, Collins (2003) used textures and compositional criteria to interpret zircon overgrowths are metamorphic and occurred ca. 525 Ma during an event that signifies the collision between Australia and India.

Orthogneisses with 780-680 Ma protoliths exposed in the Leeuwin Complex preserve Mesoproterozoic whole-rock Sm-Nd T_{DM} model ages, ranging from 1499 to 1141 Ma (McCulloch, 1987; Black et al., 1992; Fletcher and Libby, 1993; Fitzsimons, 2003; Bodorkos et al., 2016) (Fig. 3). This is considerably younger than T_{DM} model ages of orthogneisses and granitoids of the Northampton Complex (2094-2060 Ma) and suggests juvenile input (Bodorkos et al., 2016). However, the relationship between these rocks and the ca. 1090 Ma rocks in the Leeuwin Complex remains unclear, and is the subject of ongoing research (Arnoldi, 2017; Arnoldi et al., 2017) and discussion on this field trip.

Whole-rock geochemistry has been used in conjunction with geochronological data to unravel the magmatic history of the protoliths (Wilde and Murphy, 1990; Nelson, 1996; Wilde, 1999; Collins and Fitzsimons, 2001). The ca. 1090 Ma gneisses plot as syn-collisional granites on the Rb/Yb+Ta granite discrimination diagram of Pearce et al. (1984) and have S-type geochemistry, whereas the 780-680 Ma suite can be classified as A-type granites, and have a ‘within-plate’ affinity (Collins

and Fitzsimons, 2001). The 790-680 Ma protoliths have been interpreted to have been emplaced in an extensional environment relating to the break-up of Rodinia (Wilde, 1999).

Geochronology of Perth Basin Basement Well Intersections

The handful of wells drilled in the Perth Basin that intersected basement provide additional glimpses of the hidden part of the Pinjarra Orogen. Whole-rock Sm-Nd data collected from bottom-of-hole granitoids and felsic orthogneisses in five wells by Fletcher et al. (1985) and Fletcher and Libby (1993) were recalculated by Fitzsimons (2003). In the north, granitoid and felsic orthogneiss from Jurien-1 and N Yardarino-1 drill core yielded T_{DM} model ages of 2234 Ma and 2078 Ma, respectively. Felsic orthogneiss from ~3074 m in Sue-1 (drilled on the Vasse Shelf adjacent to the Leeuwin Complex), CRA CRCH-1, and Treeton DDH-1 yielded T_{DM} ages of 2040 Ma, 2002 Ma, and 1996 Ma, respectively (Fitzsimons, 2003; Bodorkos et al., 2016) (Fig. 3).

Recent SHRIMP U-Pb zircon geochronology from Sue-1 drill core indicates a complex age spectra, with an upper intercept of 1076 ± 35 Ma interpreted as the emplacement age (Bodorkos et al., 2016). A poorly-constrained lower intercept of 680 ± 110 Ma was interpreted as post-crystallisation disturbance, potentially linked to an early Cambrian (540-520 Ma) event recorded across the Pinjarra Orogen (Collins, 2003; Bodorkos et al., 2016) (Fig. 3).

In the north, basement samples from Beagle Ridge 10A and Wendy-1 have been investigated by SHRIMP U-Pb zircon geochronology (Bodorkos et al., 2016; Markwitz et al., 2017). Zircon from felsic orthogneiss in Beagle Ridge-10A yielded a weighted mean $^{207}Pb/^{206}Pb$ age of 1092 ± 27 Ma interpreted as a magmatic crystallization age (Bodorkos et al., 2016) (Fig. 3).

Zircon in a paragneiss recovered from Wendy-1 preserves rims with a $^{207}Pb/^{206}Pb$ Concordia age of 526.3 ± 12 Ma, interpreted as a metamorphic overgrowth event (Markwitz et al., 2017). Zircon cores preserve a wide range of ages, with concordant analyses ranging from 2845 ± 14 Ma (a single analysis) to ca. 1065 Ma and notable peaks at ca. 1119 Ma, ca. 1211 Ma, and ca. 1533 Ma (Markwitz et al., 2017) (Fig. 3).

The drill core geochronological data are consistent with data from the three inliers, which supports the concept that a belt of isotopically-coherent Paleoproterozoic crust occupies the full length of the Pinjarra Orogen inboard of the Leeuwin Complex (Bodorkos et al., 2016). The exception seems to be the somewhat more juvenile protoliths of the Leeuwin Complex.

Offshore extent of the Leeuwin Complex

The western extent of the Leeuwin Complex is not well constrained. Continental fragments, such as the Naturaliste Plateau and Gulden Draak, have been recognised to the west of the Leeuwin Complex (Borissova, 2002; Halpin et al., 2008; Gardner et al., 2015). Geochronology of the closest dredge samples to the Leeuwin Complex, taken over 500 km offshore on the Naturaliste Plateau, gives insights into its affinity (Borissova, 2002; Halpin et al., 2008; Gardner et al., 2015). Zircon cores from granite and felsic orthogneiss yielded LA-ICPMS U-Pb ages of returned ca. 1180 Ma, interpreted to represent emplacement age of the protoliths (Halpin et al., 2008) (Fig. 3). These authors suggested that these rocks have a stronger genetic affinity to the Albany-Fraser Orogen than the Pinjarra Orogen. Monazite and one zircon rim analysis from the same samples yielded ages of 515 ± 5 Ma and ca. 510 Ma, respectively (Halpin et al., 2008) (Fig. 3). Along with ca. 508 Ma $^{40}Ar/^{39}Ar$ ages from felsic gneisses reported by Borissova (2002), these younger ages are broadly coeval with metamorphic zircon growth in the Pinjarra Orogen, and are interpreted to represent the tectonic suture of India and Australia-Antarctica during the assembly of Gondwana (Fitzsimons, 2003; Halpin et al., 2008).

A new view of the Leeuwin Complex from aeromagnetics

The spatially restricted and disjointed nature of the coastal outcrops has hampered resolution of the structural architecture of the Leeuwin

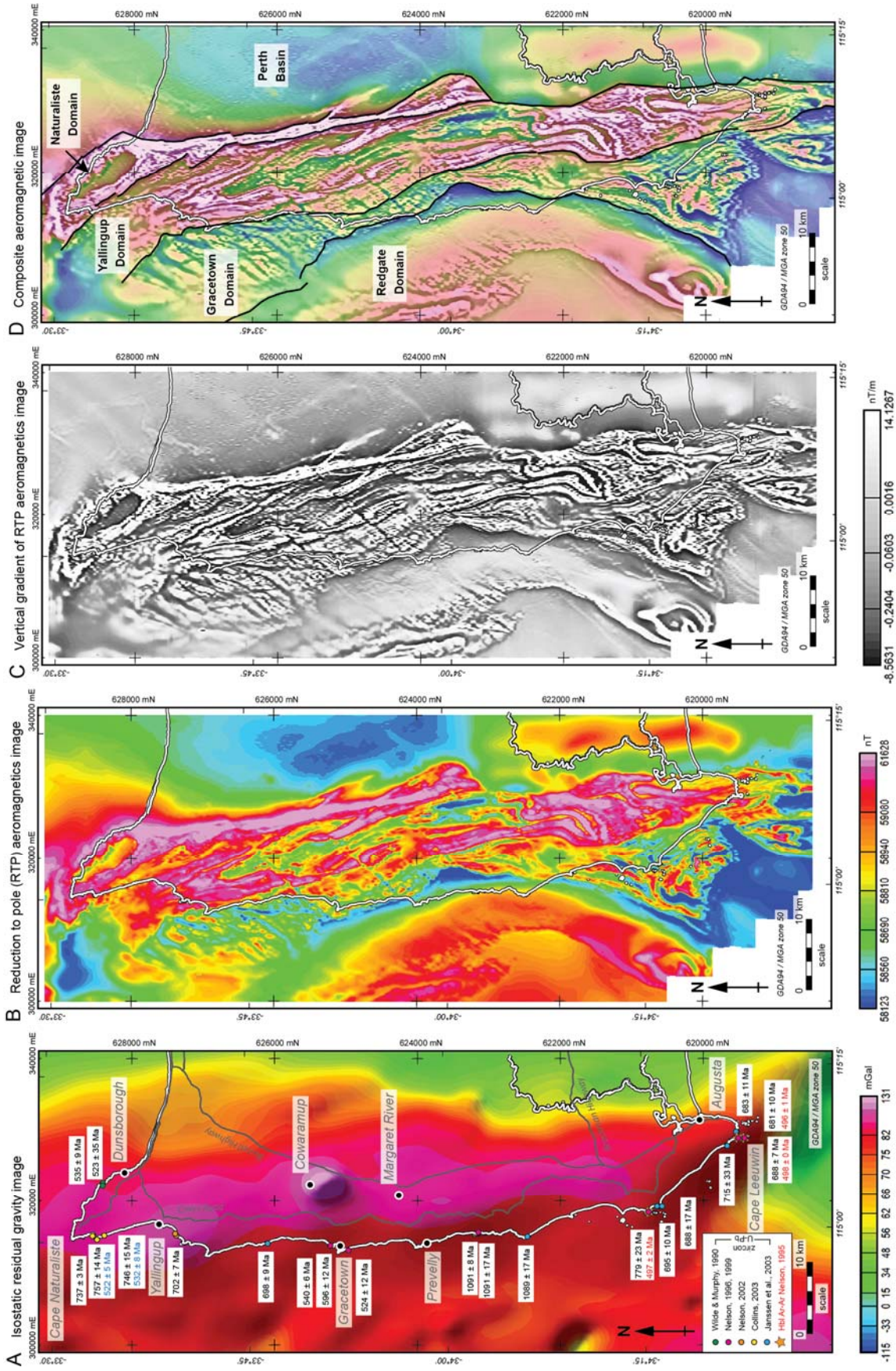

Figure 4. *A. Isostatic residual gravity image. Geochronology localities based on zircon U-Pb data from Wilde and Murphy (1990); Nelson (1996); Nelson (1999); Nelson (2002); Collins (2003); Janssen et al. (2003), and hornblende $^{40}Ar/^{39}Ar$ ages from Nelson (2005). Zircon rim U-Pb ages in blue text. B. Reduced to pole (RTP) aeromagnetics image. C. Vertical gradient of reduced to pole aeromagnetic image. D. Composite aeromagnetics image (overlay of B and C). See text for discussion of the subdivision into domains.*

Complex. This lack of context has led to difficulties in gauging the significance of outcrop-scale structures at the regional scale, and in their correlation to produce a unified deformation history of the entire Leeuwin Complex, as flagged by (Janssen et al., 2003).

The acquisition of high-resolution geophysical data (Fig. 4) by the Geological Survey of Western Australia in 2011 has provided a unique opportunity to assess the architectural make-up and nature of the ductile and brittle structures of the Leeuwin Complex in far greater detail than was previously possible (Pearce, 2014; Tucker, 2014). The aeromagnetic data reveal a wealth of regional scale fold and fault structures that were previously unknown or poorly understood due to lack of exposure and/or cover of much younger rocks. A new interpretation of the Leeuwin Complex using the aeromagnetic data and field data. This provides a context in which to place all existing legacy data as well as a framework for the tectonic development of the Leeuwin Complex and its role in the evolution of the Pinjarra Orogen.

Overview and Subdivision into Domains

New interpretations by Pearce (2014) and Tucker (2014) utilised isostatic residual gravity data (GSWA Record 2004/14) and the most recently acquired aeromagnetic survey data (survey P1244), collected in 2011 by Fugro for the Geological Survey of Western Australia (Fig. 4). The survey was flown at 60 m ground clearance, 400 m spaced east–west flight lines and 4 km spaced north–south tie lines. The isostatic residual gravity image was used to help define the position of major faults, such as the Dunsborough Fault along the eastern margin of the Leeuwin Complex, although this structure is clear enough on aeromagnetic imagery (Fig. 4). The deep-seated Dunsborough Fault juxtaposes the low and smooth magnetic signature of the Perth Basin to the east from the generally highly magnetic yet heterogeneous response of the Leeuwin Complex immediately to the west.

Aeromagnetic characteristics are variable across the Leeuwin Complex, and four distinct domains based on aeromagnetic intensity and 'texture' have been defined (Fig. 4D). From east to west, these have been named the Naturaliste, Yallingup, Gracetown and Redgate Domains, respectively. The Naturaliste Domain is characterised by NNW–SSE trending linear features of high to very-high aeromagnetic intensity. The Yallingup Domain contains well-defined continuous bands alternating between high- and low-aeromagnetic response. The Gracetown Domain has a similar appearance to the Yallingup Domain, but has lower magnetic response. The Redgate Domain is somewhat different in that it generally has a smooth aeromagnetic texture with broad gradients in magnetic intensity. Only a small portion of this latter domain is onshore, being limited to an area from Kilcarnup Beach to south of Cape Freycinet. Regional (kilometre-scale) folds and, in some cases, refolded folds are readily identifiable within in the Naturaliste, Yallingup and Gracetown Domains (Fig. 4).

The boundaries between domains are distinct and commonly truncate the folds within domains. Discrete, low-magnetic narrow linear features are clearly visible that cut across the domains obliquely (typically trending NE-SW, with minor NW-SE, E-W and N-S occurrences), displace folded bands and coincide with faults inferred from detailed mapping (Fig. 4) (Collins, 2003).

Field observations – magnetic susceptibility

Lithological and structural field mapping of accessible coastal and inland exposures of the Leeuwin Complex at 1:3,000 to 1:5,000 scale was integrated with aeromagnetic images (e.g., Fig. 5). Magnetic susceptibility measurements were made in the field to characterise their magnitude and heterogeneity within mappable geological units and 'ground-truth' the aeromagnetic imagery (Fig. 5). The complete dataset, totalling 2,920 survey points, and details of the transect locations and rock types are summarised in Fig. 6.

The *in situ* magnetic susceptibilities measured from a variety of lithologies across the Leeuwin Complex span five orders of magnitude, and approximately correlate with the full range seen in the RTP aeromagnetic image (Fig. 6). The broad division of rock types into groupings of mafic-intermediate composition, intermediate-felsic composition and felsic composition, corresponds to an approximate *in situ* field classification of ≥ 20 % mafic minerals, between 20 % and 5 % mafic minerals and ≤ 5 % mafic minerals, respectively.

The mafic-intermediate group tend to be variable mixtures of granitoid to intermediate protoliths, amphibolite and/or mafic granulite. Generally, the mafic-intermediate rocks (equivalent to grey granodiorite gneiss of Collins (2003)) possessed the highest percentage of magnetite and shows relatively homogeneous dispersion throughout the rock. The magnetite is concentrated within the restite margins of leucosome bands and/or is found as sub-euhedral mats or large porphyroblasts (0.5–15 cm) within the minor pegmatite bodies that intrude these rocks. However, minor pegmatite dykes with planar to irregular margins that are discordant to the gneissic foliation occur in all rock types, and are predominantly not magnetite-bearing and have low magnetic susceptibility. Dark grey to black amphibolite (± biotite, ± orthopyroxene, ±

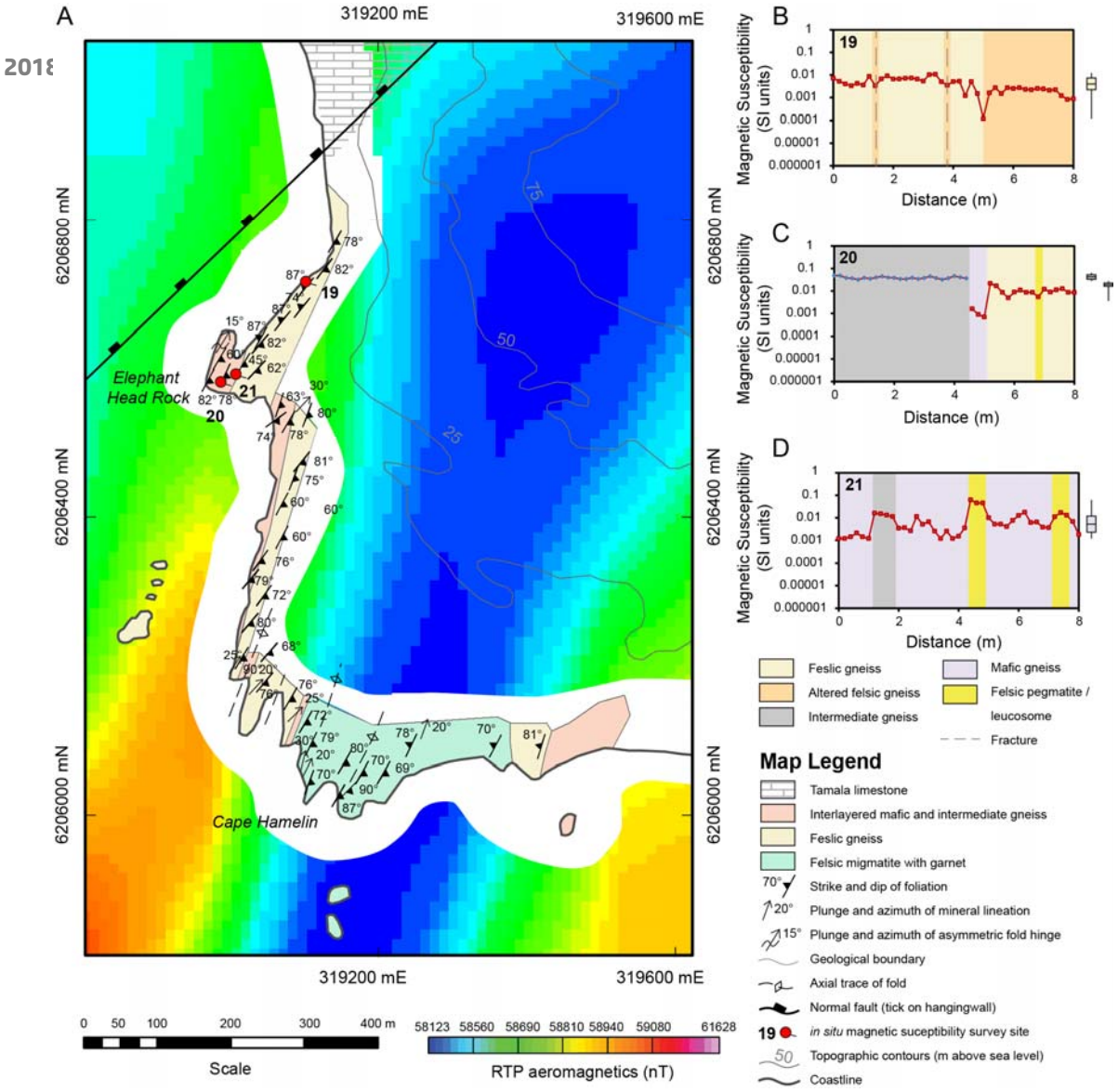

***Figure 5**. Example of the new field data that has been collected to aid interpretation of the aeromagnetics and construct the geological map of the Leeuwin Complex. A. Composite geology and RTP aeromagnetic anomaly map of the Elephant Rock to Cape Hamelin area. B-D. Transects (19-21) of in situ magnetic susceptibility measurements used to characterize different rock types as box and whisker plots (shown on right-hand side). After Tucker (2014).*

garnet) orthogneiss that is interpreted to be relict mafic dykes is present throughout the Leeuwin Complex. It varies in thickness from tens of metres to a few centimetres, and commonly preserves isoclinal fold hinges and ductile and often leucosome-filled boudinage structures. The majority of the mafic amphibolite layers throughout the Leeuwin Complex have little or no magnetite (low magnetic susceptibility), and, if present, its abundance is commonly gradational, decreasing away from the contact margins with highly magnetic units. A hornblende-plagioclase (± garnet) gneiss, referred to as the Augusta Anorthosite Complex in the vicinity of Cape Leeuwin by Myers (1990b), occurs throughout the Leeuwin Complex as an important component of the Cowaramup Gneiss (Myers, 1990c; Myers, 1994), and has a moderate magnetic susceptibility (Fig. X). Mineral abundances are consistent with these rocks having gabbro, leucogabbro and anorthosite protoliths, and they are strongly lineated in fold hinges at Sarge Bay near Cape Leeuwin (Myers, 1994).

Gneisses of intermediate-felsic grouping exhibit variable magnetite contents, often heterogeneously dispersed throughout the rock although it is also found as the primary iron oxide mineral in relatively high proportions within units of quartz-alkali feldspar gneiss and syenite gneiss. Commonly, the heterogeneity of data recorded during an *in situ* transect on rocks of this group was caused by the absence of magnetite within minor pegmatite intrusions, or cryptic magnetite stratification that does not seem associated with alteration or any discernible variance in the gneissic fabric.

Rocks of felsic character display heterogeneous magnetite distributions in a similar way to gneisses with higher proportions of mafic minerals. The granitoid gneisses that have foliations defined by characteristic discontinuous mafic schlieren (composed predominantly of biotite and hornblende) and

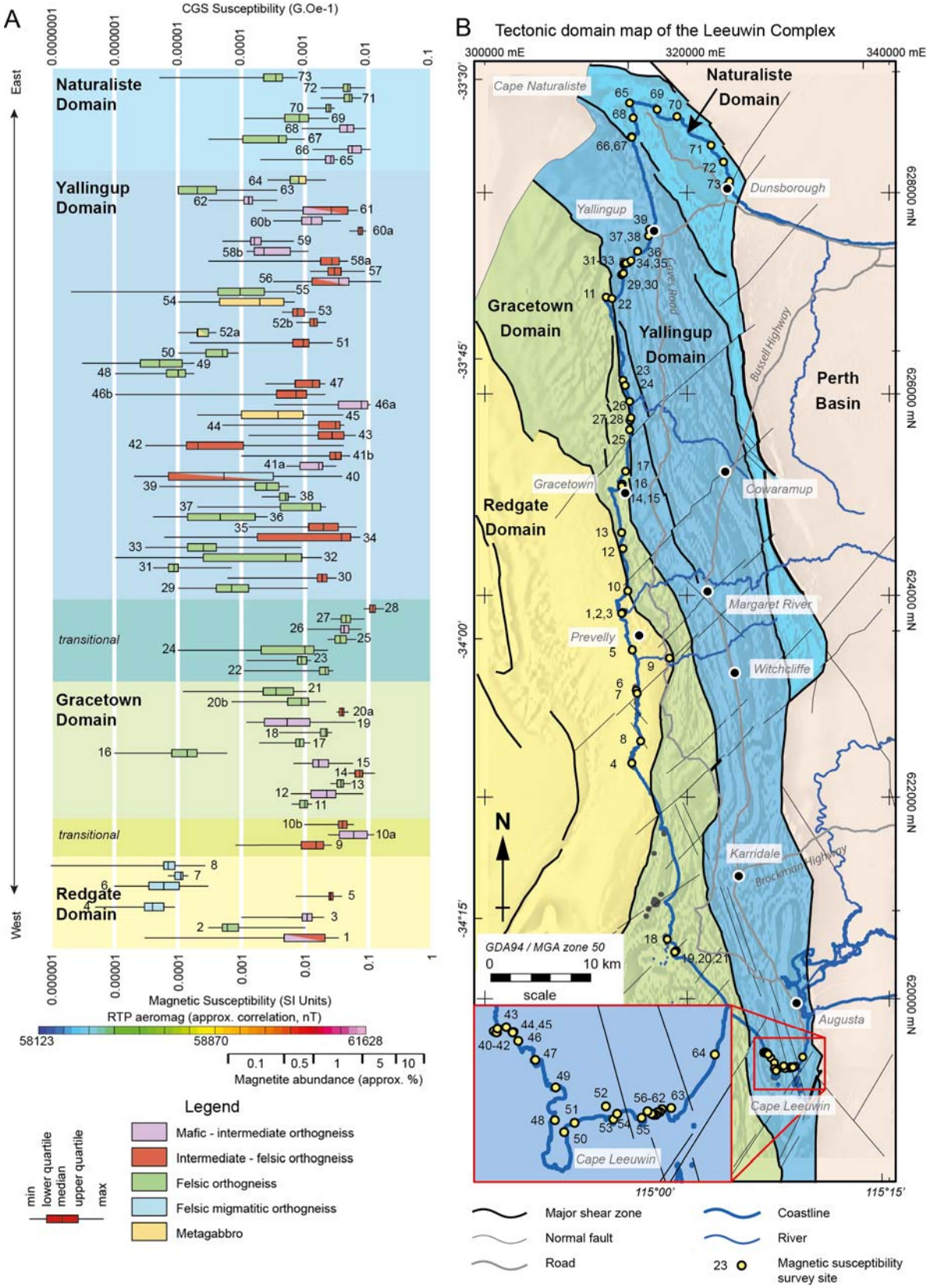

***Figure 6**. A. Box and whisker plots summarizing the in situ magnetic susceptibility of rocks of the Leeuwin Complex from 73 transects. B. A map showing aeromagnetic domains (Fig. 4d) and the locations of in situ magnetic susceptibility transects. . Data collected by Pearce (2014) and Tucker (2014).*

planar to sub-planar pegmatitic leucosome bands that have been variably recrystallised (Fig. 5) were found to have consistently low proportions of magnetite with minor concentrations associated with leucosome bands.

Felsic migmatitic (typically garnet-bearing) orthogneiss within the Redgate Domain has the lowest magnetic susceptibility of all the lithotypes, and is most probably responsible for the low RTP values along the eastern margin of the Redgate Domain (Fig. 6). Leucosomes can be garnet-bearing and typically have a lower magnetic susceptibility than the host rock. The Naturaliste Domain is dominated by felsic and mafic rock types with high measured magnetic susceptibility, which corresponds well to its aeromagnetic characteristics. Overlapping field magnetic susceptibility values means that it is difficult to unequivocally discern different rock types in the Yallingup and Gracetown Domains and their transitional zones solely from the aeromagnetic image (Fig. 6). Nevertheless, broad connections can be made between the gneiss of intermediate composition and a homogenously elevated magnetite content, similarly, a homogenously low magnetite content appears related to a seemingly less-deformed granitic gneiss (equivalent to the pink granite of Collins (2003)), and mapped outcrop patterns tend to match the relative aeromagnetic response reasonably well (e.g. Fig. 5). Felsic/granitic gneisses commonly form the headlands because they are relatively resistant to erosion, and typically weather cream, pale grey to pink.

Structural geology

Across the Leeuwin Complex, the dominant large-scale aeromagnetic banding matches layering in outcrop defined by lithological boundaries and a parallel gneissic foliation S_1 (Figs 7-9). The aeromagnetic image is dominated by N-S to NNW-NNE trending kilometre-scale folding of these bands, which correspond with folds assigned to D_2 by Janssen et al. (2003). These folds are especially prevalent in the Yallingup Domain where structural data show that they are predominantly asymmetric, sub-horizontal (in the south) to moderately N-plunging (in the north), and upright to slightly overturned to the west (Figs 8 and 9). Type 3 (hook) interference patterns seen on aeromagnetic images in the vicinity of Karridale and Witchcliffe indicate that F_2 folds are refolded resulting in NW-SE trending axial traces (Fig. 9). These are not consistent with the orientation of an F_3 fold inferred to explain systematically rotated mineral lineations in the Naturaliste Domain by Collins (2003). The F_3 of Collins is not apparent on aeromagnetic images, and its relative timing relationship with NW-SE refolds in the Yallingup Domain is unclear.

The orientation of S_1 within the Gracetown Domain is heterogeneous, with occurrences of shallow east-dipping to subhorizontal zones that are not present in the Yallingup Domain (other than locally within fold hinges) (Fig. 7). Janssen et al. (2003) reported asymmetric recumbent isoclinal folds at Deepdene Beach, with hinges plunging 30° towards 020°. These authors offered three interpretations: refolded F_1/F_2 folds; transposed F_1/F_2 in a flat-lying high strain zone; or folding during an event unrelated to F_1/F_2 at Cape Leeuwin. Even though the origin of these flat lying domains was unclear to Janssen et al. (2003), they acknowledged their significance throughout the central Leeuwin Complex (i.e., Gracetown and Redgate Domains). Shallowly east to northeast dipping S_1 with isoclinal, asymmetric recumbent folds defined by 5 cm to 3 m thick amphibolite layers within felsic gneiss are seen in outcrops from Moses Rock to Wilyabrup Cliffs. Lineations are well developed on S_1 of the felsic gneiss along this section and trend from due east to SE (Fig. 7). This down-dip orientation is at high angles to lineations elsewhere, with no clear relative timing evidence.

The Redgate Domain is dominated by a subhorizontal gneissic foliation (composite S_1/S_2?) that anastomoses on a scale of tens of metres, wrapping around lenticular lower-strain pods containing abundant asymmetric mesoscale folds of an earlier (S_1?) gneissic fabric (Myers, 1994; Harris, 2003; Janssen et al., 2003). Folds in the pods tend to be tight overfolds with axial planes that dip moderately to the east. These have been interpreted to form due to back-rotation in low strain pods within larger shear zones. (Harris, 2003). Leucosomes define ~N-S trending lineations that align with the hinges of these folds, representing sites of partial melt segregation due into axial planes during folding. Sigma-shaped porphyroclasts are not well developed in either the low-strain pods or the enveloping S_1/S_2 foliation, and so kinematics relating to the development of this fabric is equivocal. However, the asymmetry of back-rotated folds is consistent with an overall a top-to-the west sense of shear.

Assembly of the Leeuwin Complex

The Leeuwin Complex, and Pinjarra Orogen as a whole have clearly played an important role in the assembly and break-up of Rodinia and Gondwana. However, the paucity of data and poor exposure renders several possible non-unique interpretations for paleocontinental reconstructions.

The only occurrences of ca. 1090 Ma zircon U-Pb ages in the Leeuwin Complex are from within the Redgate Domain (Fig. 4a). The other domains preserve a range of zircon U-Pb ages from 779 ± 23 Ma to 524 ± 12 Ma with no clear spatial pattern (Fig. 4a). The Redgate Domain has no evidence of the ca. 800-650 Ma felsic protoliths that dominate the other domains. Combined with its different characteristics on aeromagnetic images and recent isotopic data indicating different model ages (Arnoldi, 2017),

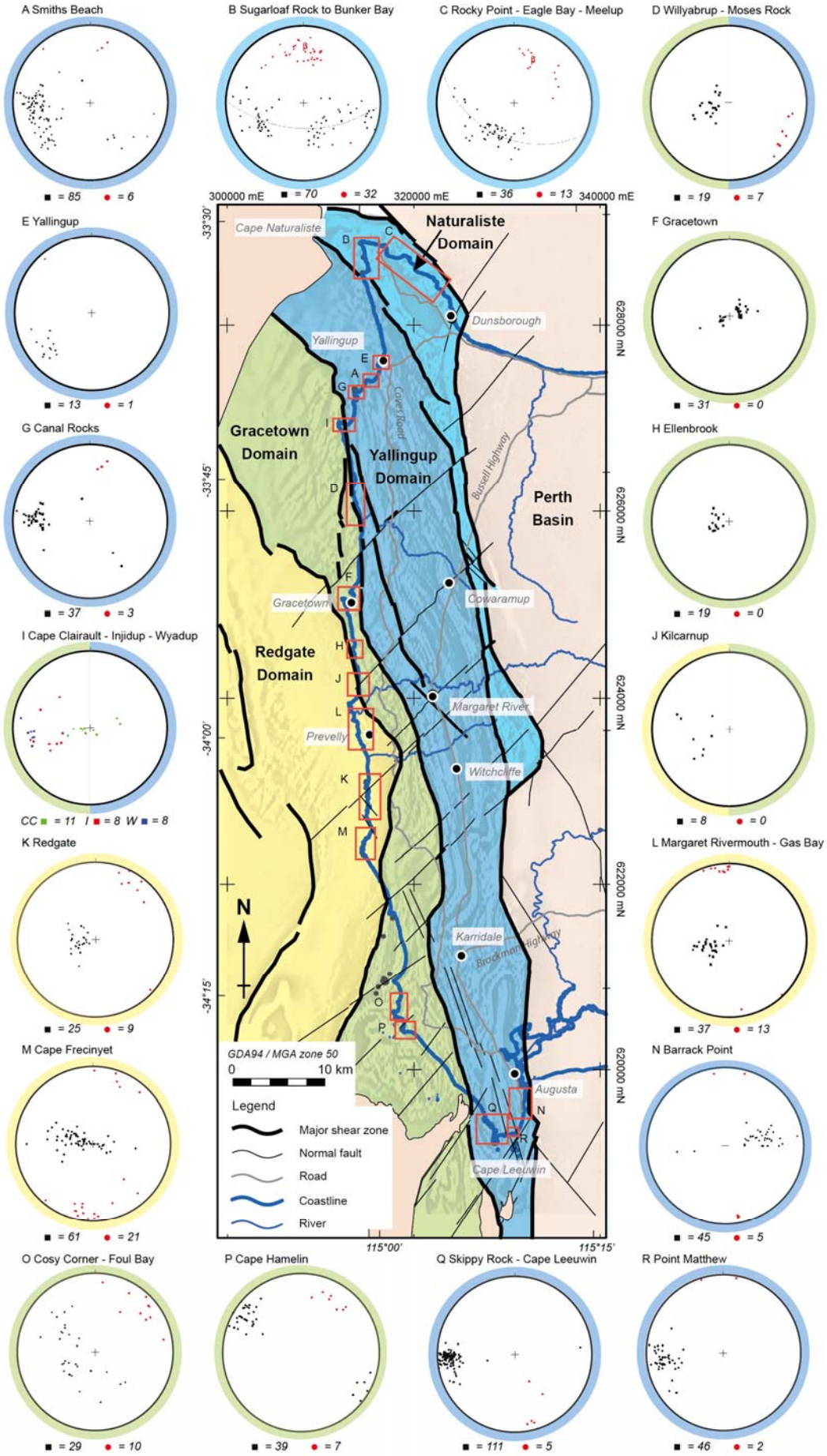
A Smiths Beach
■ = 85 ● = 6
B Sugarloaf Rock to Bunker Bay
■ = 70 ● = 32
C Rocky Point - Eagle Bay - Meelup
■ = 36 ● = 13
D Willyabrup - Moses Rock
■ = 19 ● = 7
E Yallingup
■ = 13 ● = 1
F Gracetown
■ = 31 ● = 0
G Canal Rocks
■ = 37 ● = 3
H Ellenbrook
■ = 19 ● = 0
I Cape Clairault - Injidup - Wyadup
CC ■ = 11 I ■ = 8 W ■ = 8
J Kilcarnup
■ = 8 ● = 0
K Redgate
■ = 25 ● = 9
L Margaret Rivermouth - Gas Bay
■ = 37 ● = 13
M Cape Frecinyet
■ = 61 ● = 21
N Barrack Point
■ = 45 ● = 5
O Cosy Corner - Foul Bay
■ = 29 ● = 10
P Cape Hamelin
■ = 39 ● = 7
Q Skippy Rock - Cape Leeuwin
■ = 111 ● = 5
R Point Matthew
■ = 46 ● = 2
300000 mE
320000 mE
340000 mE
-33°30'
-33°45'
-34°00'
-34°15'
628000 mN
626000 mN
624000 mN
622000 mN
620000 mN
115°00'
115°15'
Cape Naturaliste
Naturaliste Domain
Dunsborough
Yallingup
Gracetown Domain
Yallingup Domain
Perth Basin
Busselt Highway
Caves Road
Gracetown
Cowaramup
Redgate Domain
Margaret River
Prevelly
Witchcliffe
Karridale
Brockman Highway
Augusta
Cape Leeuwin
N
GDA94 / MGA zone 50
0 10 km
Legend
Major shear zone
Normal fault
Road
Coastline
River

Figure 7 *(previous page). Structural data from the Leeuwin Complex. Map shows aeromagnetic domains identified from Fig. 4. A-R. Stereographic projections of structural data from field areas shown by red boxes on map. Pole to dominant foliation shown in black and lineations shown in red on stereographic projections. Data collected by Pearce (2014) and Tucker (2014).*

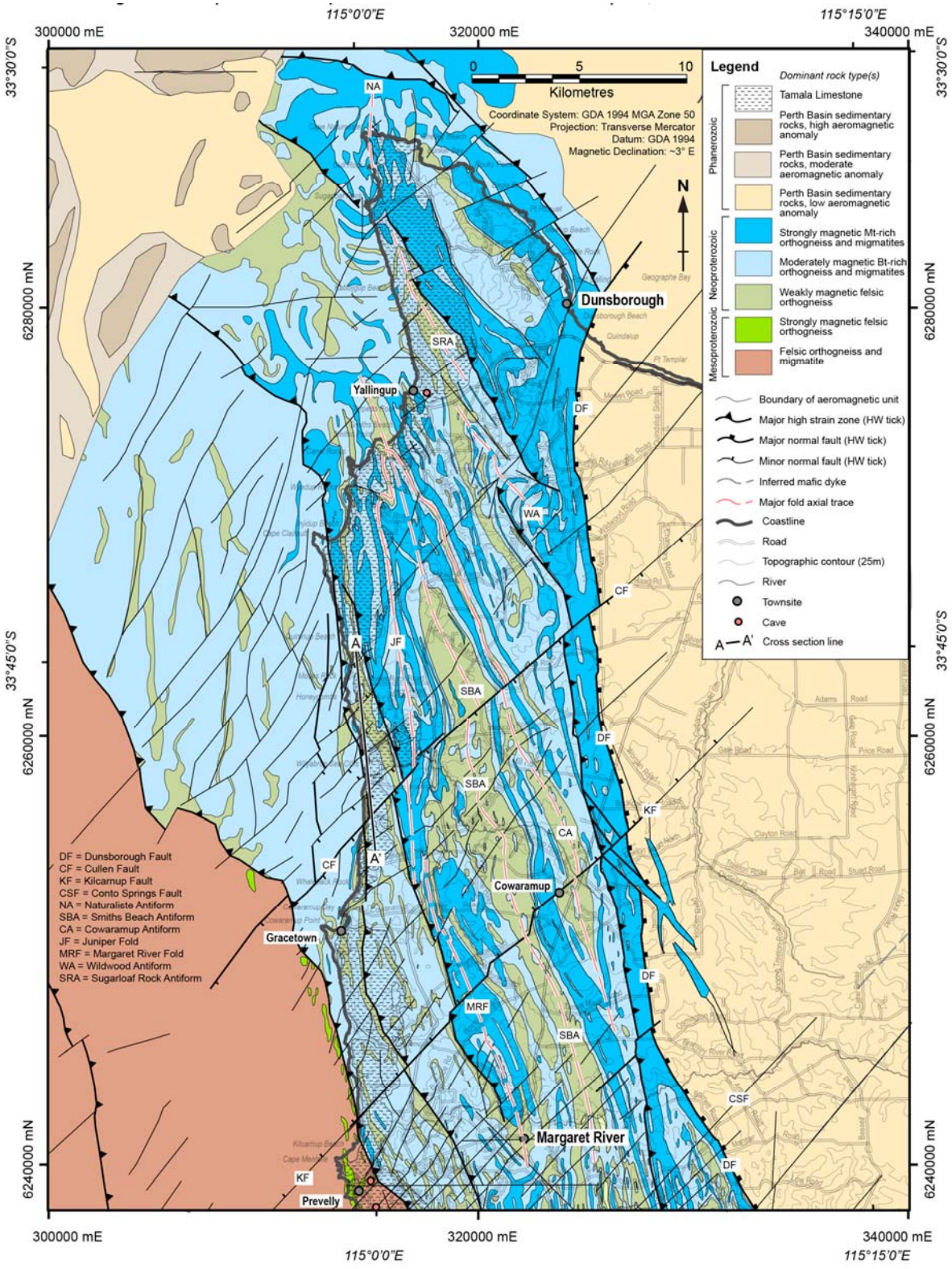

Figure 8*. Interpreted geological map of the northern Leeuwin Complex. After Pearce (2014).*

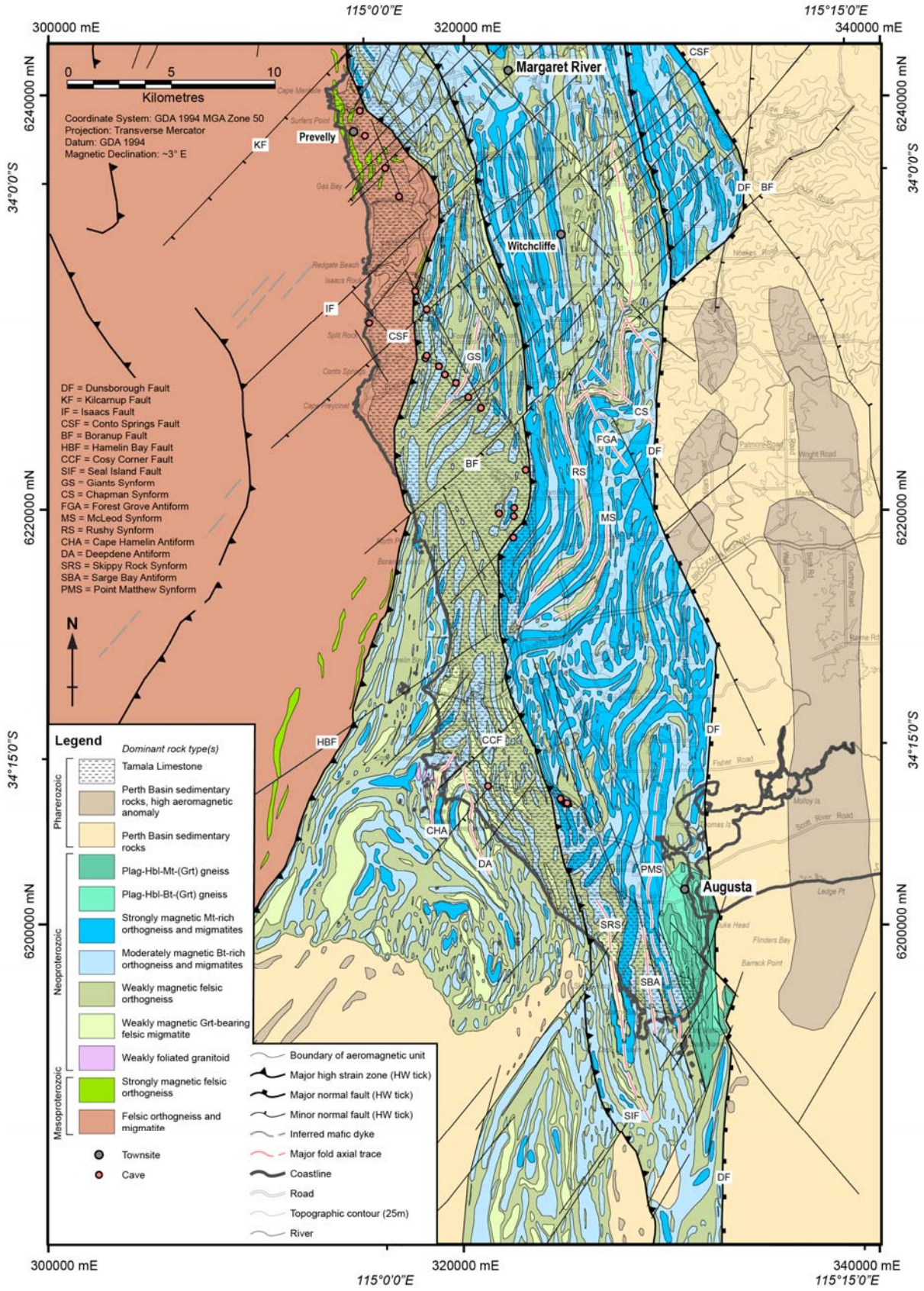

***Figure 9**. Interpreted geological map of the southern Leeuwin Complex. After Tucker (2014).*

it is plausible that the Redgate Domain represents a separate terrane (tentatively named here as the Redgate Terrane), whereas the protoliths of the Gracetown, Yallingup and Naturaliste Domains share an affinity, potentially allowing them to be grouped (tentatively named as the Margaret River Terrane). All domains in the Leeuwin Complex record the 540-520 Ma event, consistent with the assembly of the domains by this time.

The boundaries between the aeromagnetic domains are not exposed, which precludes further investigation of their nature. Nevertheless, the truncation of S_1 and F_2 (e.g., the boundary between the Yallingup and Naturaliste Domains) suggests that they are high strain zones that post-date F_2 folding. However, their temporal relationship with NW-SE refolds in the Yallingup Domain is unclear. The fact that the boundary between the Regate and Gracetown Domains follows the trend of nearby S_1 suggests that this boundary is sub-parallel, likely flat-lying to gently east-dipping. This suggests that the Margaret River Terrane is structurally overlies the Redgate Terrane at the current level of exposure. What is not currently possible to determine, however, is whether or not the Redgate Terrane is present beneath the Margaret River Terrane throughout the Leeuwin Complex, and if it does, whether it is continuous with basement rocks of the Vasse Shelf, with which it shares T_{DM} model age and zircon U-Pb age characteristics.

The well-developed lineations in the vicinity of Wilyabrup plunge gently to the east in the down-dip direction, which is unusual in the Leeuwin Complex. The close proximity of Wilyabrup to the boundary between the Gracetown and Yallingup Domains means that it is plausible that these lineations (L_2?) are linked to motion along the domain boundary zones, indicating dip slip with either normal or thrust sense in the context of simple shear. However, the shear sense of the Domain boundaries remains elusive due to lack of reliable kinematic indicators, yet has significant implications for the assembly of the Leeuwin Complex into its current configuration. A thrust motion would be consistent with the west-verging asymmetry of F_2 folds, and could imply that the domains were juxtaposed late during the D_2 event. Alternatively, domain boundaries had normal dip-slip kinematics, exhuming the Redgate Domain akin to a metamorphic core complex. A third option is motion with a significant transcurrent component, in which lineations do not form parallel to transport direction. However, but this is difficult to reconcile with the curved traces of the boundaries on the regional scale. The lack of kinematic indicators could be explained by strain partitioning during deformation in the presence of melt rather than a lack of non-coaxial component of deformation. This is supported by abundant field evidence of synkinematic leucosomes.

New zircon U-Pb geochronology, REE and Lu-Hf isotope data from the Leeuwin Complex

A Curtin Honours thesis by Arnoldi (2017) aimed to provide insights into the crustal evolution and tectonic development of the Leeuwin complex via new U-Pb geochronology, REE, and Lu-Hf isotope data from three garnet-bearing orthogneiss samples targeted from the central and southern Leeuwin complex {Arnoldi, 2017 #1473} (Fig. 10). One sample is from Redgate Beach within the Redgate Domain, and the other two samples are from Skippy Rock and Cape Naturaliste, respectively, in the Yallingup Domain. SHRIMP zircon U-Pb analysis of the Redgate Beach sample yielded a crystallisation age of 1095 ± 11 Ma (Fig. 10), which is consistent with the interpreted magmatic age of 1091 ± 8 Ma by Nelson (1999) for the same rock unit from Redgate Beach. Steep HREE patterns in zircon from this sample are consistent with garnet-absent zircon growth. A single spot from a CL-dark zircon rim yielded 553 ± 16 Ma and flat HREE profile, interpreted to be a garnet-present metamorphic overgrowth (Fig. 10).

Orthogneiss from Cape Leeuwin yields a more precise crystallisation age of the granite protolith at 692 ± 7 Ma, which is consistent with the interpreted magmatic protolith age of 681 ± 10 Ma by Nelson (1999) for the same rock unit from Cape Leeuwin. Two spots from CL-dark rims yield ages ca. 527-537 Ma (Fig. 10).

U-Pb analyses of CL-dark zircon rims from garnet-rich gneiss from Skippy Rock provides the most precise age of 524 ± 6 Ma for the timing of metamorphism (Fig. 10), which is comparable with 522 Ma age which was suggested for peak metamorphism in the Leeuwin Complex by a number of authors. The flatter M-HREE pattern for these zircon rims indicates growth in the presence of garnet in these rocks during the early-Cambrian metamorphic event (Fig. 10). A large spread in U-Pb data and elevated LREE is preserved by for zircon cores in this sample, potentially indicating partial resetting and alteration of a ca. 700 Ma protolith during metamorphism (Fig. 10).

Zircon Lu-Hf isotope analysis shows that the Redgate Domain sample is distinct from the two samples from the Yallingup Domain (Fig. 10). All data plot along linear arrays that can be accounted for by ancient Pb-loss during metamorphism. Data from the Redgate Beach and Skippy Rock samples plot below CHUR, reflecting evolved crustal packages, whereas the magmatic protolith of the Cape Leeuwin orthogneiss is clearly more juvenile (Fig. 10). A key observation is that the ~1095 Ma and ~700 Ma magmatic rocks do not lie along the same crustal evolution trend, indicating that these two periods of magmatism are distinctly different from one another (Fig. 10). Addition of a juvenile component is required to explain the Lu/Hf composition of the ~700 Ma Cape Leeuwin orthogneiss protolith, possibly in an intracontinental or back-arc rift setting. Furthermore, the ~1095 Ma protoliths from

Redgate Beach yielded an average hafnium depleted mantle model age (T_{DM}^2) of 2.2 Ga, whereas the ~700 Ma protoliths are paired with average model ages of 1.5 Ga for Skippy Rock and 1.8 Ga for Cape Leeuwin (Fig. 10). The combination of U-Pb and Lu/Hf analyses clearly reinforce that the Redgate Domain has a distinctly different crustal evolution to the other younger, more juvenile Gracetown, Yallingup, and Naturaliste Domains that comprise the bulk of the exposed Leeuwin Complex. However, the Redgate Domain shares isotopic characteristics with crystalline basement below the Perth Basin and inliers of the Pinjarra Orogen (Fig. 10).

Tectonic evolution of the Leeuwin Complex

The nature of the juxtaposition of domains in the Leeuwin Complex is pertinent to a key outstanding issue surrounding the Pinjarra Orogen: whether the multiple events reflect repeated reworking of an orogen that was already assembled by ca. 1090 Ma (Ksienzyk et al., 2012), or distinct allochthonous domains evolved separately prior to their juxtaposition at ca. 525 Ma during Gondwana assembly (Fitzsimons, 2003). In this context, the ca. 1090 Ma Redgate Domain could be a truly allochthonous terrane, i.e., an exotic crustal block that was tectonically emplaced from elsewhere. Alternatively, the Margaret River Terrane is para-autochthonous. The 780-690 Ma protoliths were emplaced magmatically into pre-existing ~1090 Ma crustal rocks with T_{DM} of ~2 Ga (now the Redgate Domain and Basement to the Vasse Shelf), and subsequently formed a locus for ductile deformation during Gondwana assembly. The latter option is consistent with the A-type granite geochemistry of the Margaret River Terrane protoliths, and corroborates extensional setting for their emplacement suggested by Wilde and Murphy (1990). Multiple lines of evidence need to be considered to address this problem, and models need to satisfy the available data from igneous and metamorphic geochronology, igneous geochemistry, detrital provenance of metasedimentary units, paleomagnetic data, geophysical data, structural architecture and deformation history. This will be a topic for discussion during the field trip. Key points to consider include:

- 1090 Ma intrusion of granitoids with ca. 2 Ga T_{DM} at Redgate;
- Metamorphism of paragneiss in the Northampton Complex at 1090-1020 Ma;
- 790-680 Ma intrusion of granitoids, most juvenile input = breakup of Rodinia;
- Mafic dykes and big folds in Leeuwin post-date 790-680 Ma protoliths;
- 1090 Ma and 790-680 Ma rocks are spatially separate, with 1090 Ma rocks structurally beneath;
- Orogen-wide tectonometamorphism ca. 525 Ma = collision of Australia and Greater India (Gondwana);
- Mundine Well and Northampton Complex dyke swarm paleomagnetic poles align.
- Northampton Complex paragneiss with detritus sources ca. 1400, 1300, and 1190 Ma, needs to be deposited prior to metamorphism at ca. 1090 Ma.
- D_3 structures = transpression due to oblique docking of India?

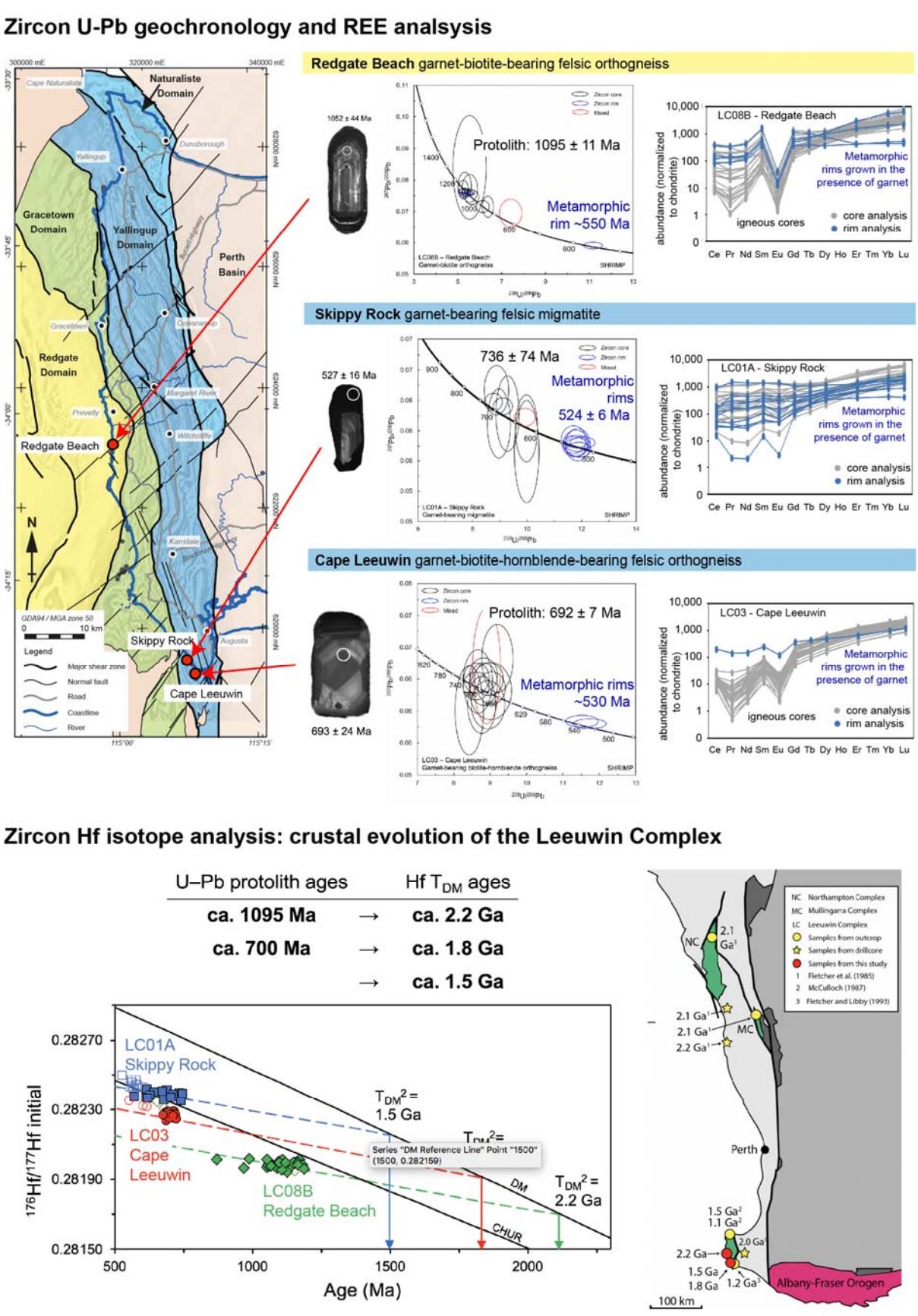

Figure 10. *New SHRIMP zircon U-Pb geochronology, LA-ICPMS REE and Lu-Hf isotope analyses from the central and southern Leeuwin Complex. After Arnoldi (2017).*

Gondwana Break-up: Rifting of the Perth Basin and Southern Rift System

By comparison to the amalgamation of Gondwana, rifting events that eventually led to the break-up of Gondwana and development of a passive margin along the western coast of Western Australia are fairly well constrained. Intracontinental rifting initiated as early as the Ordovician to form the N-S trending Perth Basin (Harris, 1994b). The current onshore expression of the Perth Basin ranges for over 1,000 km from the southern margin of Australia to beyond Geraldton, where a somewhat arbitrary boundary is made with the Southern Carnarvon Basin to the north (Fig. 1). Rifting probably initiated along the basin-bounding, N-S Darling Fault, which nucleated on a pre-existing deep-seated ductile shear zone (Darling Fault Zone) (Dentith et al., 1993; Harris,

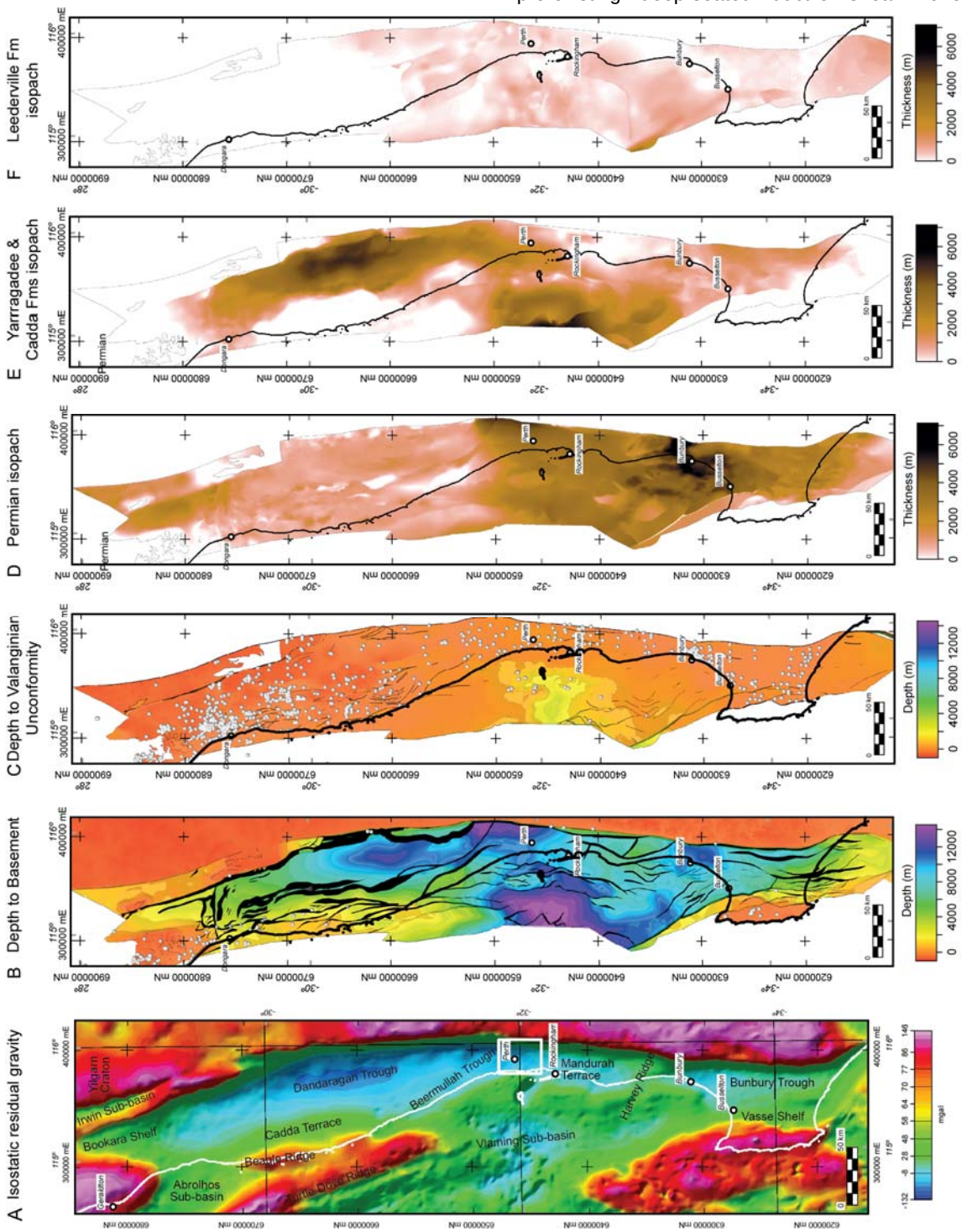

***Figure 11**. A Gravity anomaly image, B-C surface depth maps, and D-F isopach maps from a 3D model of the Perth Basin showing its structural and stratigraphic architecture. After Olierook et al. (2015c).*

1994b). The Perth Basin opens to Australia's passive margins to the south and west. The development of the southern rift system along the southern margin of Australia is summarised by (Totterdell et al., 2000; Totterdell and Bradshaw, 2004). Rifting initiated during the Late Jurassic, initially with along a NW-SE azimuth, when fluvial and lacustrine sediment-filled half grabens developed in the Bight and Druntoon Basins (Willcox and Stagg, 1990). This was followed by thermal subsidence phase in the Early Cretaceous as a NNE-SSW-oriented extensional regime was established (Willcox and Stagg, 1990; Totterdell et al., 2000). Accelerated rifting and breakup was diachronous along the southern margin, initiating in the west near the India-Antarctica-Australia triple junction at ca. 90-87 Ma, systematically migrated eastwards, concluding in entire margin breakup ca. 45 m.y. later (Sayers et al., 2001; Halpin et al., 2008; Direen, 2011). The southern rift system has been influenced by deep-seated pre-existing basement structures throughout basin evolution, particularly NW-SE trending shear zones (Teasdale et al., 2003; Totterdell and Bradshaw, 2004). Commencement of sea-floor spreading is defined by the earliest magnetic anomaly in the Bight region, which occurred at ca. 83 Ma (Sayers et al., 2001), which was followed by thermal subsidence and establishment of a passive margin.

The Perth Basin is subdivided into sub-basins of various trends and areal extent, reflecting depocentres and basin highs that developed at different times throughout the history of the Perth Basin (Cockbain, 1990; Harris, 1994b; Mory and Iasky, 1996; Crostella and Backhouse, 2000; Song and Cawood, 2000) (Fig. 11). Three main rift phases have been identified in the Perth Basin: these are Rift I during the early Permian (ca. 290 Ma); Rift II-1 in the earliest Jurassic (ca. 200 Ma); Rift II-2 during the mid- to late Jurassic (ca. 165 Ma) leading to continental break-up during the Early Cretaceous (Song and Cawood, 2000). A semi-continuous record of siliciclastic sedimentation during these times is preserved in most of the Perth Basin (Olierook et al., 2015c) (see Fig. 11 for examples). Post-break-up sedimentation is minor onshore but is significant offshore where deposition continues today (Olierook et al., 2015c).

Phases of subsidence and fill have been punctuated by regional unconformity-forming events, recognised by gaps in the paleontological record, thermal maturation, and geometric relationships interpreted from seismic surveys (Iasky, 1993; Crostella and Backhouse, 2000) (Fig. 11).

Southern Perth Basin

For this field trip, we will focus on the southern Perth Basin because of its spatial position relative to the Leeuwin Complex and potential for access to outcrops, but also because it is the most proximal to the site of three-way break-up of eastern Gondwana: the triple junction between Australia, Antarctica and Greater India. The main features of the southern Perth Basin are the Bunbury Trough and Vasse Shelf, which form a N-S trending graben-half graben system between the Yilgarn Craton and Leeuwin Complex (Fig. 11). The Bunbury Trough contains up to ca. 10 km sedimentary fill, and the deepest parts of the Vasse Shelf preserves 3-4 km of sedimentary rocks (Iasky, 1993; Olierook et al., 2015c) (Fig. 11). The earliest known sedimentary rocks in the southern Perth Basin are the Permian Sue Group, which were deposited contemporaneously with sediments in the small, en echelon, NW-SE trending Collie, Yilga and Boyup Basins on the Yilgarn Craton (Playford et al., 1976; Iasky, 1993; Harris, 1994b) (Fig. 1). Deposition of the Sabina Sandstone, Lesueur Sandstone, Cattamarra Coal Measures, Yarragadee Formation and Parmelia Group followed prior to formation of the Valanginian Unconformity due to uplift and erosion during continental break-up (Iasky, 1993; Olierook et al., 2015c). Other notable unconformities in the onshore southern Perth Basin formed at the end of the Permian, localised to the Vasse Shelf and Harvey Ridge (Iasky, 1993; Olierook et al., 2015c), and the Cenozoic reactivation of faults in the Bunbury Trough that produced a topographic high known as the Blackwood Plateau (Czarnota et al., 2013; Barnett-Moore et al., 2014).

Subsidence and uplift have been controlled by activity of multiple sets of faults in different orientations. The N-S trending Dunsborough, Busselton and Darling Faults bound the Vasse Shelf and Bunbury Trough. These and other similarly-oriented subsidiary faults (e.g., Darradup Fault) dominated the architecture of these depocentres (Iasky, 1993). Minor NE-SW trending faults (e.g. Sabina Fault) were recognised is seismic surveys in the vicinity of Whicher Range on the Vasse Shelf and NW-SE trending faults offshore north of Bunbury (Iasky, 1993; Iasky and Lockwood, 2004).

Exhumation associated with unconformity-forming events has been quantified for the southern and central Perth Basin using sonic log data (Olierook and Timms, 2016). This reveals that Permian strata on the Vasse shelf underwent locally variable exhumation during the Permian-Triassic of between 400 and 1,500 m, which was probably caused by differential footwall block uplift during a rifting event (Olierook and Timms, 2016). The Triassic-Jurassic event resulted in average of 500 m net exhumation during, and post-Early Cretaceous exhumation averaged 600 m.

The record of rifting in the Leeuwin Complex

The Dunsborough Fault that defines the eastern margin of the Leeuwin Complex is parallel to a highly magnetic band in the Naturaliste Domain in the northern part of the Leeuwin Complex (Figs 4, 8, 9). In the vicinity of Witchcliffe, the Dunsborough Fault cuts obliquely across the Naturaliste Domain

in a NE-SE orientation, and is parallel with the strike extension of the boundary between the Naturaliste and Yallingup Domains further south (Figs 4 and 9). This is plausible evidence that the segments of the Dunsborough Fault nucleated on pre-existing ~N-S domain boundaries in the Leeuwin Complex, hard linked by segments of other known orientations in the Perth Basin. This interpretation corroborates the suggestion by Harris (1994b) that Proterozoic shear zones were reactivated during rifting associated with the development of the Perth Basin.

Sets of NE–SW, NNW-SSE and minor E–W faults are conspicuous on aeromagnetic images as discrete narrow domains of low total magnetic intensity that truncate and displace aeromagnetic banding (Fig. 4). Several of the larger NE-SW trending faults have been named, including the Cullen, Kilcarnup, Isaacs, Contos Springs, and Boranup Faults (Figs 8 and 9). Faults typically manifest as kinks in the modern coastline and are mostly obscured by sandy bays and/or river mouths (Figs 8 and 9).

These structures are consistent with faults identified by Collins (2003) between Dunsborough and Cape Naturaliste, and have identical orientations to faults in the Perth Basin (Iasky, 1993; Olierook et al., 2015b). These faults are assumed to have a normal dip slip sense of displacement. However, the exact timing of their formation is not constrained. Mapping along a coastal section between Gracetown and Moses Rock shows significant changes in elevation of the unconformity between the basement gneisses of the Leeuwin Complex and overlying Quaternary Tamala Limestone across these faults (Fig. 12). However, no evidence of displacement within the Tamala Limestone has been observed, suggesting that some fault movement occurred during erosion of the unconformity surface, but have been inactive since the Quaternary.

Bunbury Basalt – Flow Geometry and Timing with Respect to Continental Break-up

Initial break-up of eastern Gondwana between Greater India and Australia has been constrained to ca. 137-136 Ma using recent plate reconstructions and palynological biozones from underlying strata (Gibbons et al., 2012; Jones et al., 2012). The oldest confirmed sea floor spreading anomaly in the Indian Ocean adjacent to Australia is chron M10, which is ca. 134 Ma (Williams et al., 2013). Extrusion of a series of lava flows and deeper level sheet intrusions, collectively known as the Bunbury Basalt, has been associated with the break-up event (Playford et al., 1976; Frey et al., 1996; Coffin et al., 2002) (Fig. 13). The Bunbury Basalt is the only volcanic activity in the entire Perth Basin, and only occurs in the Bunbury Trough (Olierook et al., 2015b) (Fig. 13). Recent reassessment of the age of the Bunbury Basalt via high-precision plagioclase $^{40}Ar/^{39}Ar$ plateau ages from nine samples has revealed that the Bunbury Basalt erupted in three distinct phases, at 136.96 ± 0.43 Ma, 132.71 ± 0.43 Ma and 130.45 ± 0.82 Ma (Olierook et al., 2016) (Fig. 13). These data confirm that the oldest Bunbury Basalt flows were synchronous with continental break-up. The Bunbury Basalt is geochemically similar to E-MORB, and could have been produced from a patch of enriched shallow mantle beneath the southern Perth Basin by decompression melting related to passive rifting between Greater India and Australia (Frey et al., 1996; Olierook et al., 2016). This magmatism could also have been one of the first vestiges of the Kerguelen plume, which has been responsible for long-lived magmatism forming multiple oceanic plateaux, and is now situated in the Southern Ocean (Frey et al., 1996; Olierook et al., 2015a; Olierook et al., 2016) (Fig. 13).

The Bunbury Basalt is mostly covered by siliciclastic sediments, and outcrops in the vicinity of the town of Bunbury, at Black Point on the south coast, and sparse outcrops in river beds elsewhere (Fig. 13). A recent 3D model of the Bunbury Basalt developed from a survey of >30,000 wells and analysis of aeromagnetic data illustrates that lava flows up to 100 m thick were mainly confined to two N-S draining paleovalleys and their tributaries in the Bunbury Trough (Olierook et al., 2015b) (Fig. 13). The Donnybrook paleovalley (containing 47 km^3 of lava) was situated close to the Darling Fault, and flows were even draped over the Yilgarn Craton along its tributaries (Olierook et al., 2015b). The Bunbury paleovalley (with 43 km^3 of lava) meandered centrally within the Bunbury Trough (Fig. 13). Both systems indicate south-to-north fluvial drainage at the time of continental break-up, which contrasts to the east-to-west drainage patterns of modern river systems in the Perth Basin (Olierook et al., 2015b). Deeper mafic intrusions that are inferred to be affiliated with the Bunbury Basalt are intersected in four wells in the vicinity of the Busselton Fault (Fig. 13), and their exact geometry is unconstrained.

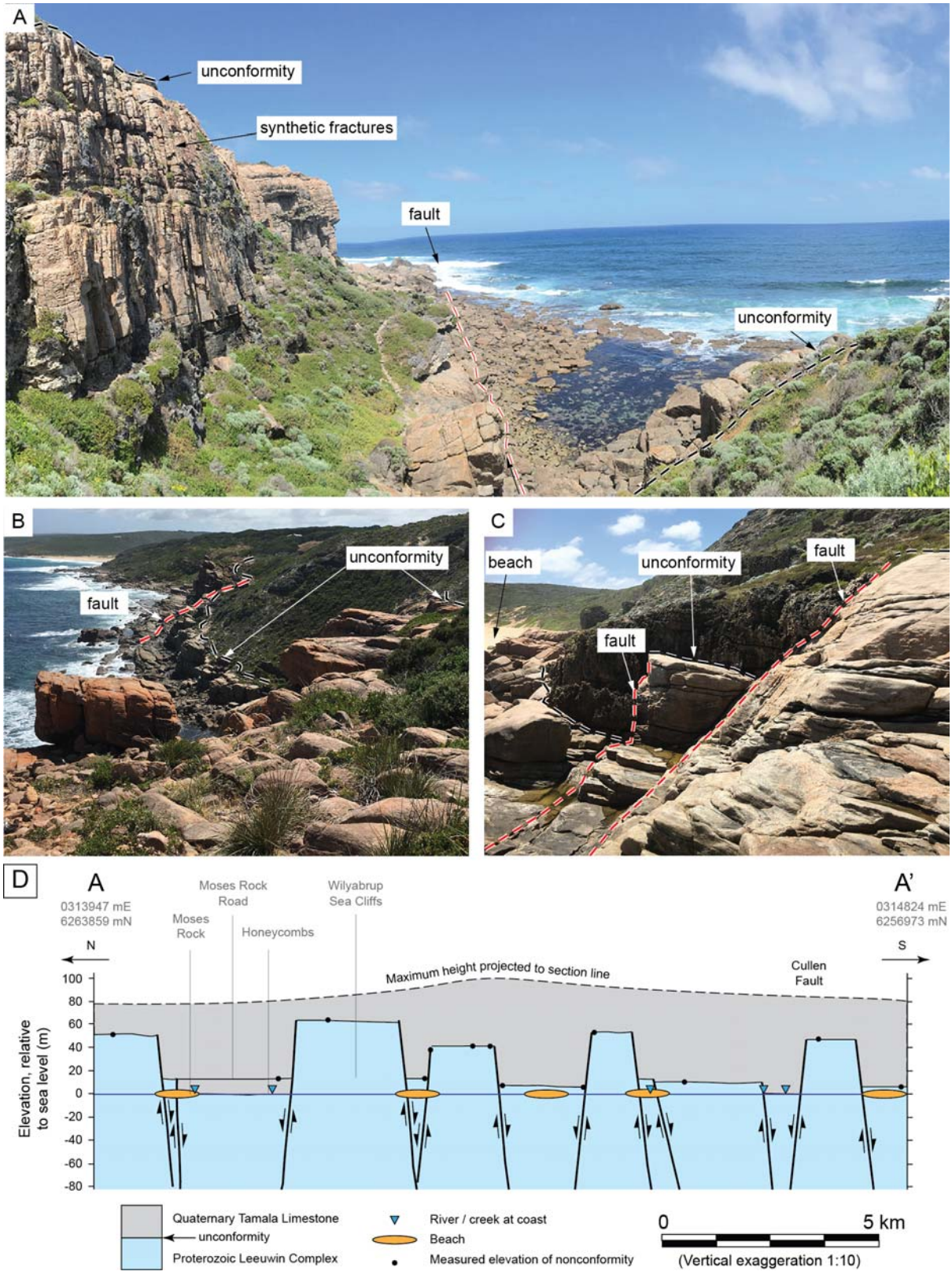

Figure 12. *Field photographs of normal faults in the Leeuwin Complex. A. ~40 m down throw to the northwest, north of Wilyabrup Cliffs. Viewing southwest. 0314890 mE, 6258900 mN. B. Significant topography on the Tamala Limestone nonconformity, Wilyabrup Cliffs, viewing north. 0314725 mE, 6257587 mN. C. 4 and 5 m throw faults, south of Wilyabrup Beach, viewing northeast. 0314270 mE, 6260640 mN. D. Cross section after Pearce (2014) to show the relationship between the faults in the Leeuwin Complex and the elevation of the nonconformity overlain by the Quaternary Tamala Limestone, along line A-A' in Fig. 8.*

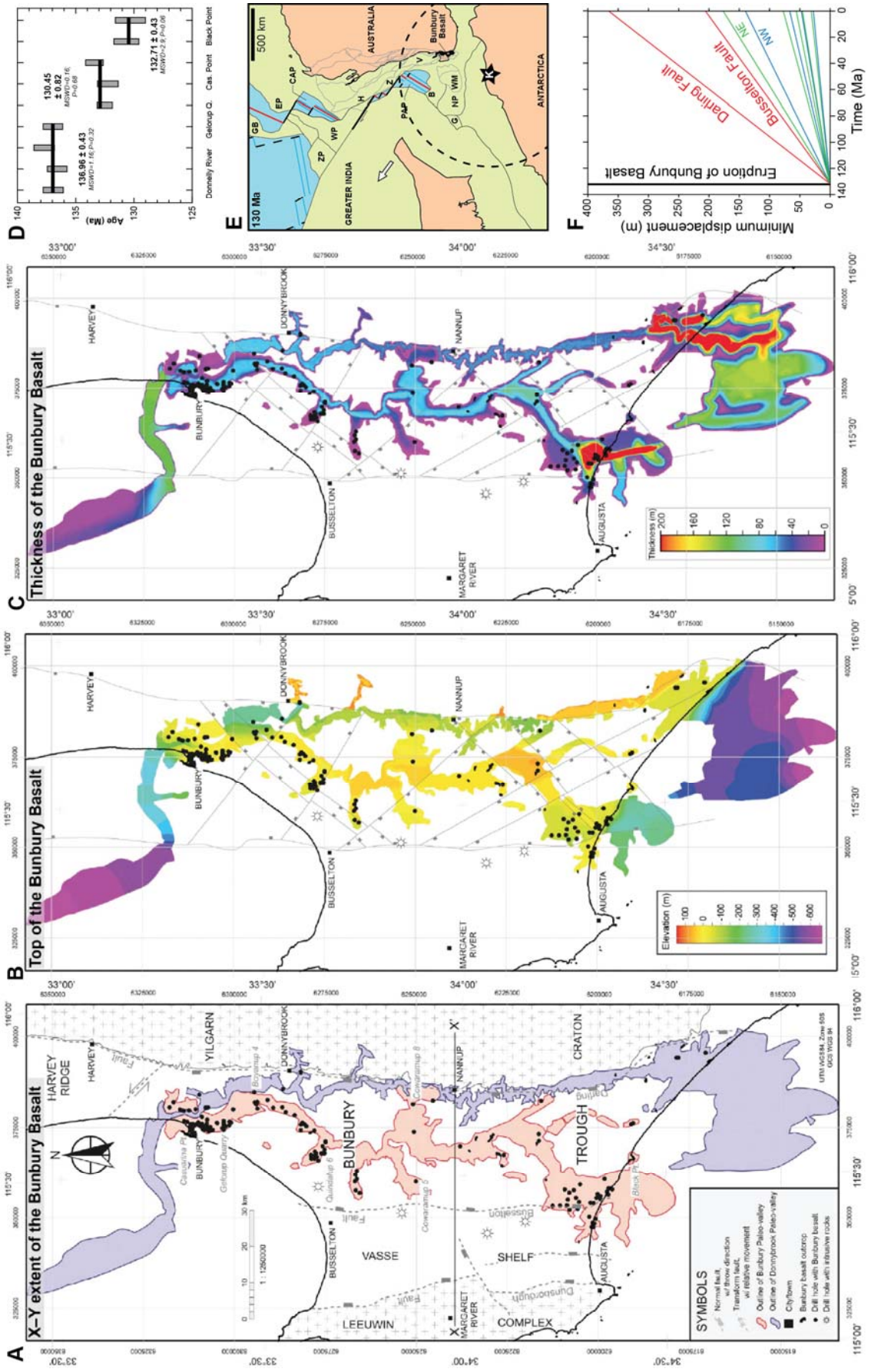

Figure 13. *The geometry and age of the Bunbury Basalt flows. A. The aerial extent of the flows, mostly confined to the Bunbury and Donnybrook paleo-valleys and their tributaries. B. Variation in the elevation of the top of the flows and inferred faults. C. Thickness of the Bunbury Basalt. D. $^{40}Ar/^{39}Ar$ age data. E. continental reconstruction at 130 Ma. F. Graph of post-Bunbury Basalt displacement of faults. After Olierook et al. (2015b) and Olierook et al. (2016).*

Offsets of the Bunbury Basalt flows seen in the 3D model have been used to newly identify NE-SW and NW-SE trending faults in the Bunbury Trough (Olierook et al., 2015b) (Fig. 13). These faults record throws of ca. 30-175 m, whereas the Darling and Busselton Faults have post-flow throws of 370 m and 210 m, respectively (Fig. 13). Mean slip rates integrated over the interval since emplacement of the Bunbury Basalt 2.8 and 1.6 m/Myr for the Darling and Busselton Faults, respectively, and <1.4 m/Myr for subordinate NE and NW trending faults. This indicates N-S trending Darling and Busselton Faults are long-lived structures, and fault activity was polymodal in the southern Perth Basin since the Cretaceous.

Where are the rifted correlatives of the Leeuwin Complex now?

The distinctive ages, metamorphic history, and geophysical characteristics of the Leeuwin Complex and the Albany-Fraser Orogen play an important role in tectonic reconstructions of Gondwana. However, the location of Antarctica's counterparts to these tectonic units is not abundantly clear, and reconstructions are not unanimously agreed upon (Fig. 14). Paleo-continent reconstruction has been attempted by many researchers using various approaches over the years (Norvick et al., 2001; Fitzsimons, 2003; Veevers et al., 2007; Boger, 2011; Williams et al., 2011; White et al., 2013; Aitken et al., 2016; Morrissey et al., 2017; Tucker et al., 2017). Previous reconstructions have placed variable emphasis on matching the geology. Valid reconstructions need to consider matches of the positions major pre-existing structures, geophysical anomalies, sedimentary basins, as well as the tectonic (P-T-t) histories and detrital provenance histories of the rocks themselves. Some previous reconstructions have suffered from correlation issues due to poor geological constraints, particularly from Antarctica. It is clear that rigorous reconstruction requires consideration of continental motion on a spherical body, and needs to be consistent with sea-floor spreading and extensional structures of the intervening basin(s), which are taken into account using G-Plates. However, a solution that satisfies all of these criteria is yet to be found.

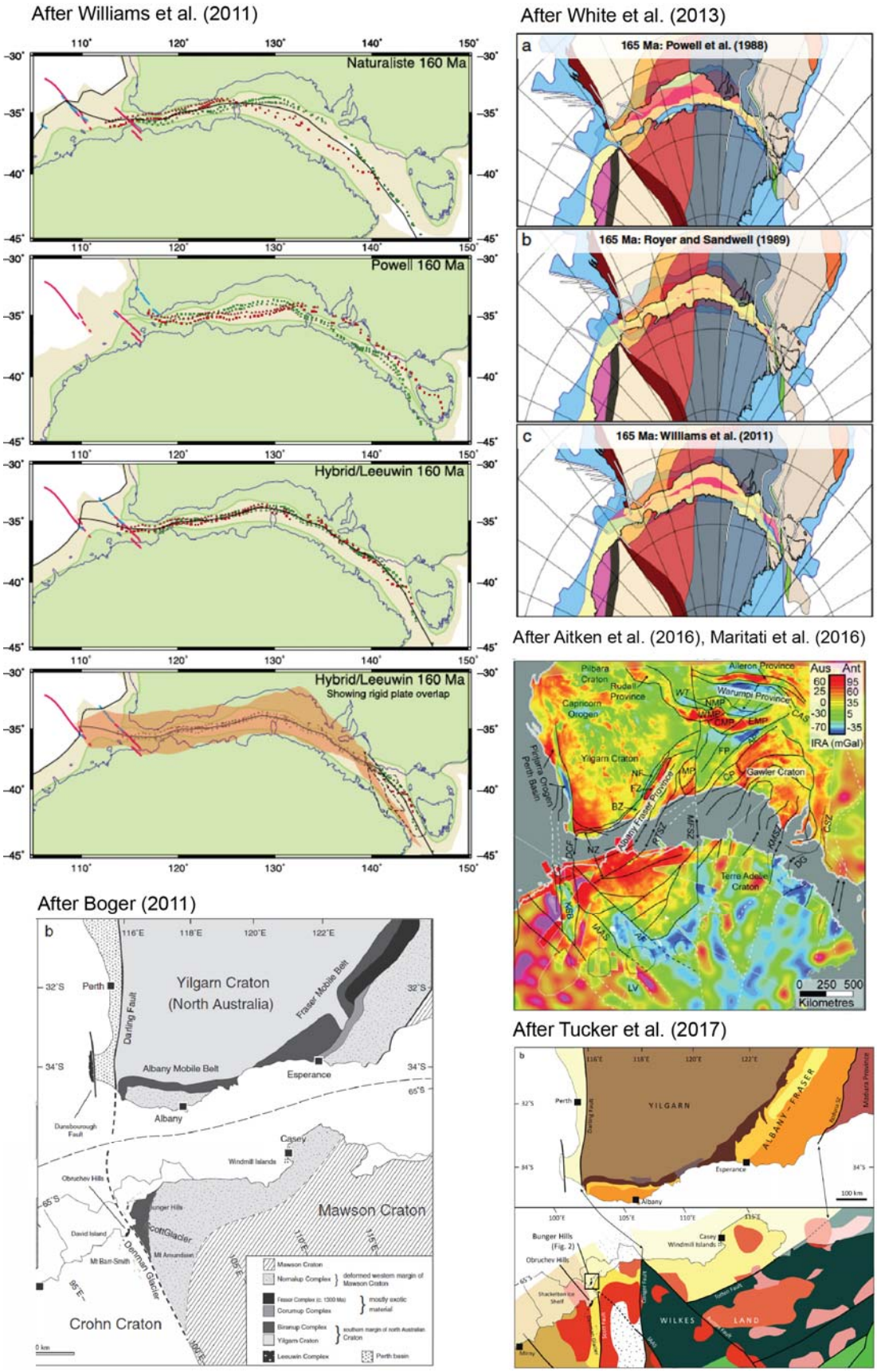

Figure 14. *A selection of different plate reconstructions that highlight discrepancies of the correlation between Australia and Antarctica.*

Field localities

Cape Leeuwin, Yallingup Domain, Leeuwin Complex

How to get there

Continue driving south on Leeuwin Road from Augusta. Parking places along this road are close to several localities of interest, including (from east to west) Augusta Boat Harbour, Point Matthew, Ringbolt Bay, Sarge Bay and Cape Leeuwin. Localities at Quarry Bay, Skippy Rock and Skippy Rock Carpark can be accessed from Skippy Rock Road, which is unsealed.

Specific Hazards

- *Keep alert for large waves that may surge over smooth rock surfaces that slope into the water. Rocks near the water are renown for being particularly dangerous at Skippy Rock Carpark.*
- *Take extra care when walking on large boulders that may move underfoot.*
- *Skippy Rock can be accessed on calm days via a sand spit. Keep a watchful eye on the tide and swell if you plan to go there.*

Geology

The region comprises gneisses of compositions that are interleaved at various scales, but typically on the order of tens to hundreds of metres. Protoliths include porphyritic granite (Cape Leeuwin), granite, anorthosite, gabbro, leucogabbro, collectively known as the Augusta Anorthosite Complex (Myers, 1990b) (Figs 15 and 16). Protolith crystallisation ages are ca. 680 Ma. Dark green to black amphibolites are present, ranging from thin (less that one centimetre wide) discontinuous and isoclinally folded ribbons (e.g., at Skippy Rock, Fig. 15C), to units that are tens of metres thick (e.g., at Ringbolt Bay, Fig. 16C). Anorthosite and some felsic gneisses are garnet-bearing (Fig. 16F). Felsic pegmatites range from planar dykes that cross cut other structures (e.g., at Ringbolt Bay), boudinaged dykes parallel with S_1, (e.g., at Ringbolt Bay, Fig. 16G), to irregular clots that can contain angular blocks of country rock (e.g., at Sarge Bay, Fig. 16D-E).

A distinctive garnet-bearing gneiss occurs at Skippy Rock (Figs. 15B, 17). Lineations defined by strings of garnet porphyroblasts in this rock plunge moderately to the northeast (Fig. 7). Coronas of plagioclase(?) and muscovite occur around garnet in this rock. Zircon cores in this rock preserve a spread of U-Pb ages (Fig. 10). This contrasts to the relatively even-textured 692 ± 7 Ma garnet-hornblende-biotite-bearing felsic orthogneiss at Cape Leeuwin (Figs. 16A, 18). Nevertheless, zircon grains in both rocks preserve metamorphic rims indicating that they both experienced early Cambrian high-grade metamorphism.

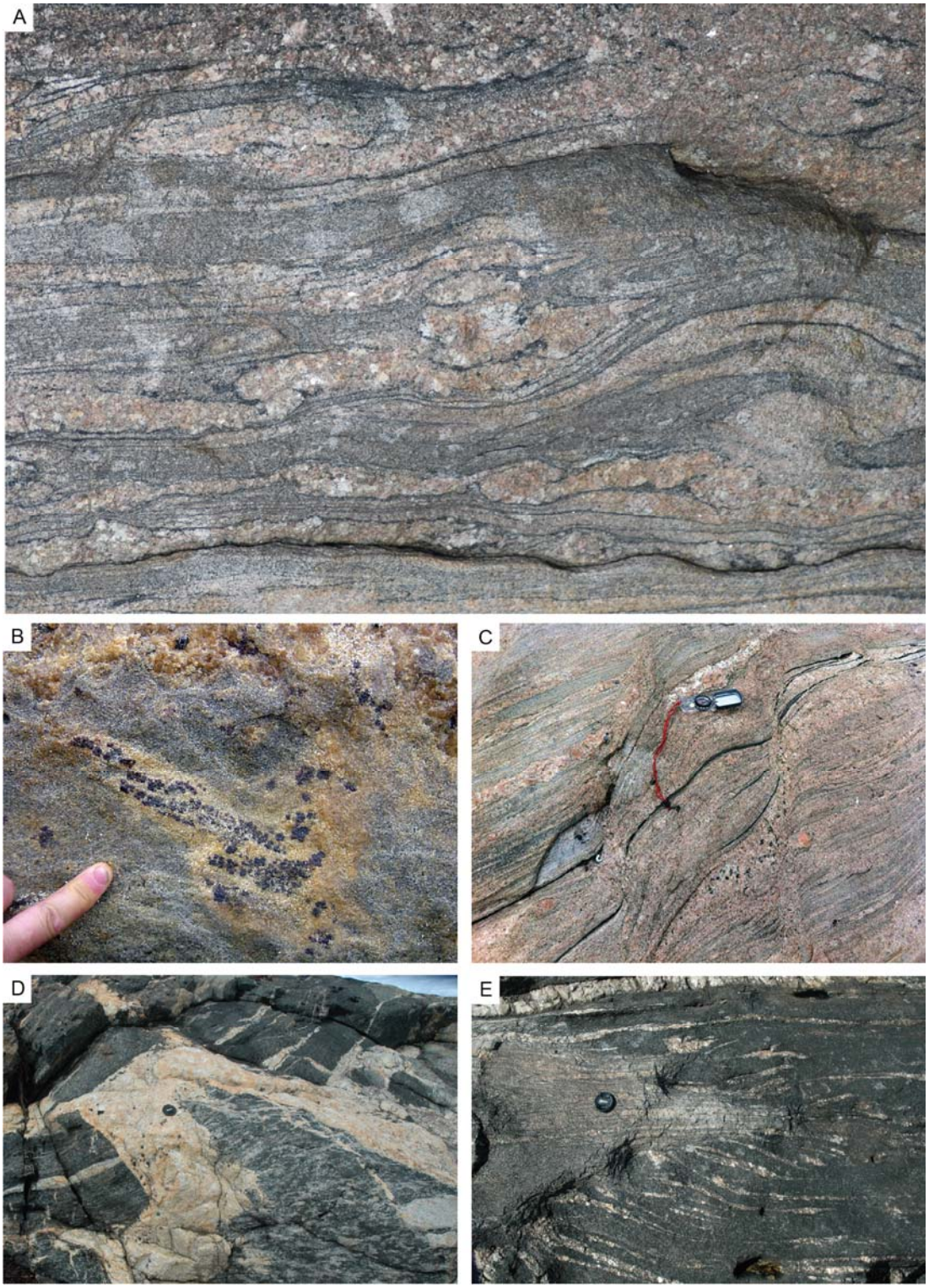

***Figure 15**. Field photos from Skippy Rock and Skippy Rock Carpark. A. Tight to isoclinal folds in felsic gneiss and leucosomes. B. Lineation defined by garnet porphyroblasts at Skippy Rock, 0327567 mE, 6196902 mN. C. Felsic gneiss with small-scale shear zone displacing centimeter-thick amphibolite layers and leucosomes, with leucosomes formed along small-scale shear zones in mixed /intermediate gneiss, east of Skippy Rock, 0327787 mE, 6196875 mN. D. Plagioclase-pyroxene pegmatite intruding gabbro and anorthosite gneiss, Skippy Rock Carpark. E. Hinge of meso-scale isoclinal fold in felsic gneiss with leucosomes developed in surrounding mafic gneiss.*

Small to medium scale isoclinal folds with steeply plunging hinges are particularly apparent at Skippy Rock Carpark, and have been assigned to (assigned to D_1, Janssen et al. (2003)) (Fig. 15A, E). These are within the limbs of NNW-trending, gently plunging upright folds (assigned to D_2 by Janssen et al. (2003)) on a 500-1000 m scale. The outline of Seal Island to the south of Point Matthew defines a sheared hinge of an F_2

fold. Anorthosite L-tectonites have developed in the hinges of these folds due to constrictional strain. Lineations from these rocks vary from ~5° S to ~25° NNE. Orthopyroxene-bearing pegmatites occur on fold limbs, which Myers (1990b) suggested is indicative of folding at granulite facies conditions.

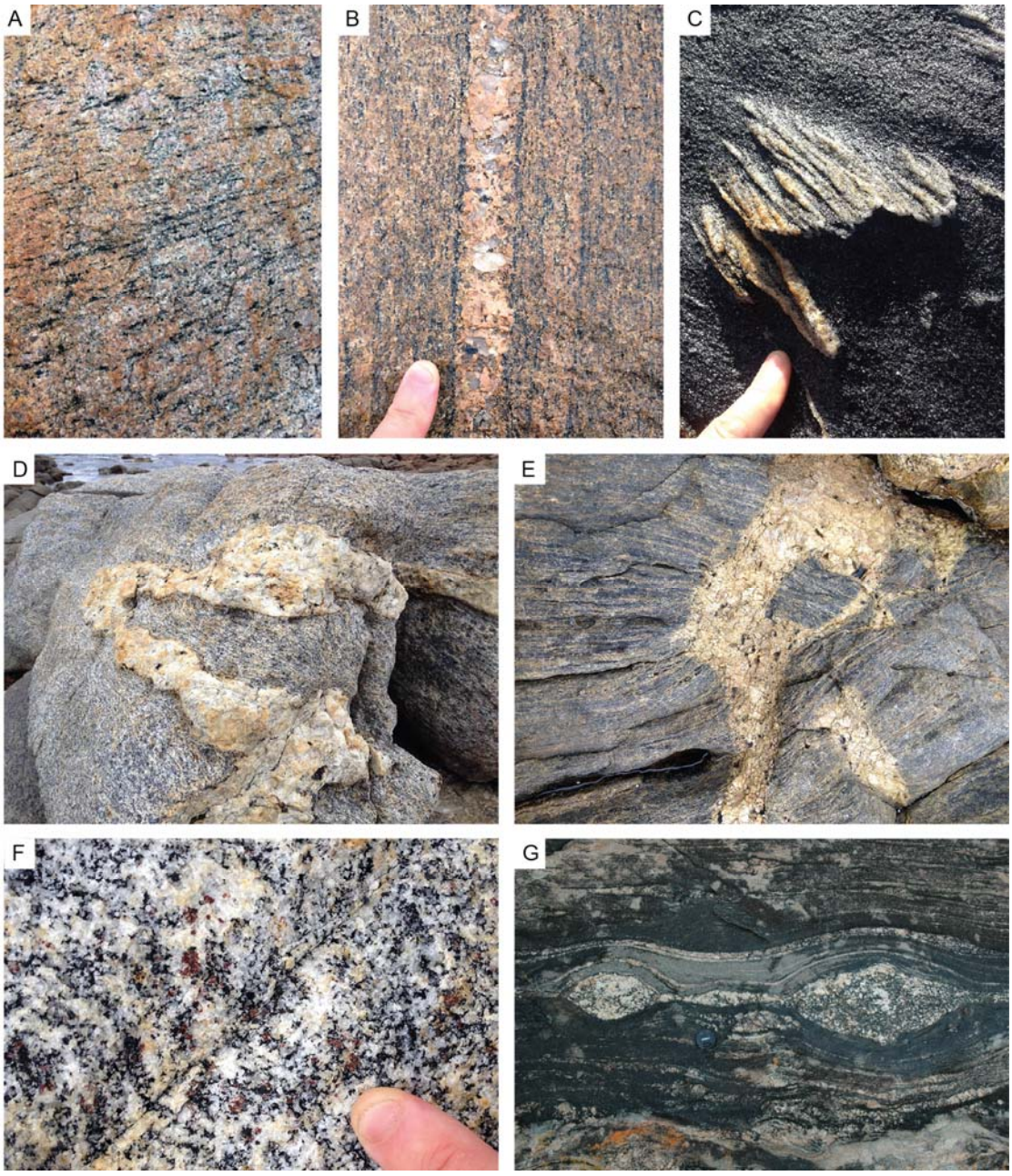

***Figure 16**. A. Foliated granitoid, Cape Leeuwin, 0328682 mE, 6195133 mN. B. Felsic gneiss with planar leucosomes bound by dark restitic domains, parallel to S_1, Sarge Bay, 0329528 mE, 6195402 mN. C. Folded quartz veins in amphibolitic gneiss, Ringbolt Bay. D. Quartz-k feldspar-magnetite pegmatite intruding strongly-lineated (L-tectonite) plagioclase-hornblende-garnet anorthositic gneiss, Sarge Bay, 0329580 mE, 6195448 mN. E. Quartz-k feldspar-magnetite pegmatite intruding intermediate gneiss, Sarge Bay, 0329492 mE, 6195375 mN. F. Plagioclase-hornblende-garnet gneiss, Sarge Bay, 0329580 mE, 6195448 mN. G. Boudinaged pegmatite in intermediate to mafic gneiss at Ringbolt Bay. Image courtesy of Steven Reddy.*

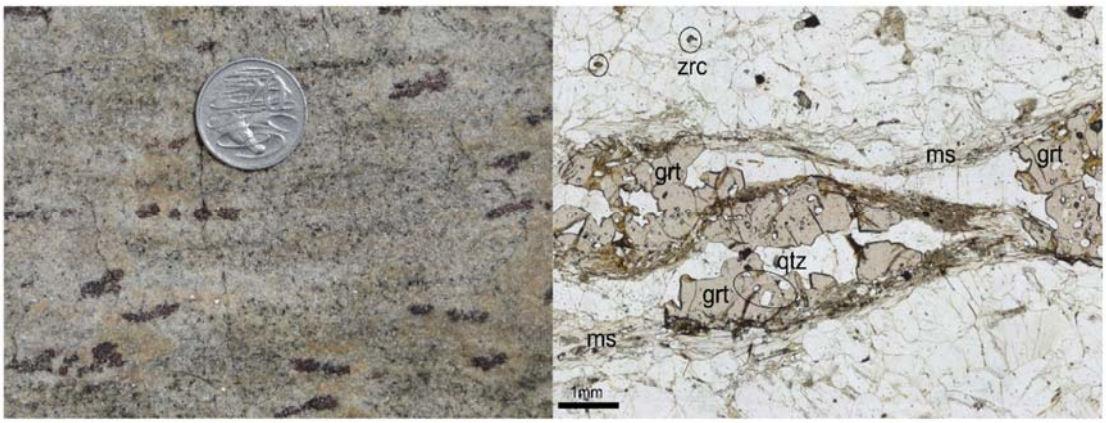

***Figure 17**. Garnet-bearing migmatite from Skippy Rock. Sample LC01A of Arnoldi (2017). Zircon grains extracted from this sample preserve cores with a spread of U-Pb ages from ca. 700 to ca. 600 Ma, thick metamorphic overgrowths at 524 ± 6 Ma, and a Hf T_{DM} age of ca. 1.8 Ga (Fig. 10).*

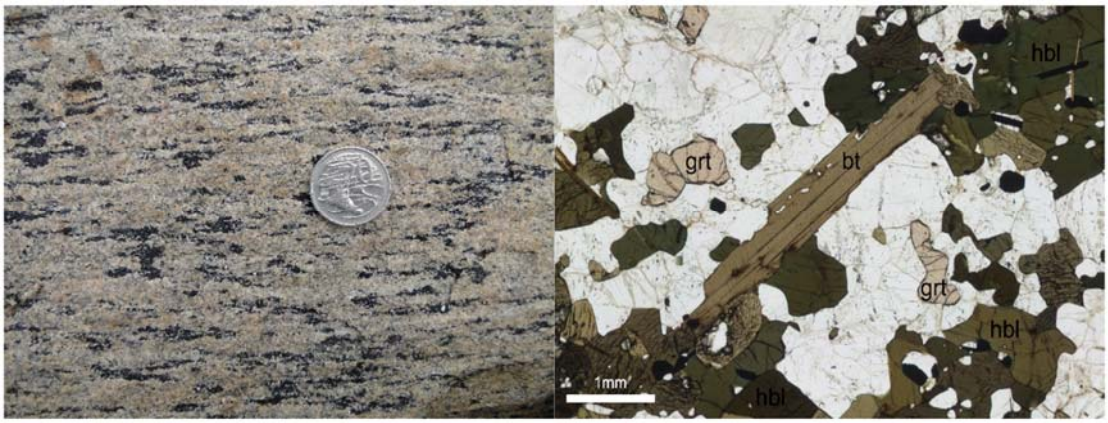

***Figure 18**. Garnet-hornblende-biotite-bearing orthogneiss from Cape Leeuwin. Sample LC03 of Arnoldi (2017). Zircon grains extracted from this sample preserve a U-Pb protolith age of 692 ± 7 Ma, ca. 530 Ma metamorphic rims, and a juvenile Lu/Hf signature with a Hf T_{DM} age of ca. 1.5 Ga (Fig. 10).*

Points for discussion

- **Folding history:** How are the small-scale isoclinal folds and large-scale upright folds linked?
- **Setting:** What was the tectonic setting for the magmatic intrusions?
- **Metamorphism:** Are there any indicators of changes in metamorphic conditions that can be linked to the structural history?

Redgate Beach, Redgate Domain, Leeuwin Complex

How to get there

From Caves Road, take Redgate Road to the coast. Continue to the carpark at the end of the road. Public toilets are available here. Take one of the tracks down to the rocky headland north of Redgate Beach.

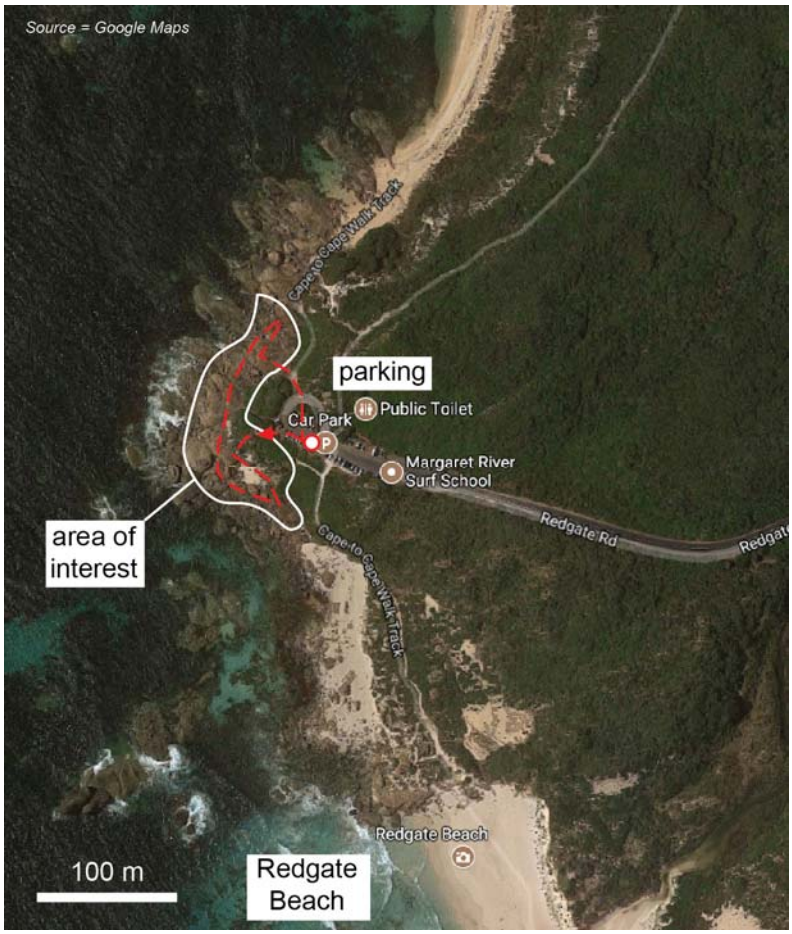

Specific Hazards

- *Waves may surge over rocky pavements at high tide or in a significant swell.*
- *Take extra care climbing and walking over boulders.*
- *Redgate Beach is renown for being dangerous in big swells, and lives have been lost in the past.*

Geology

At Redgate, the garnet-bearing gneiss of the Redgate Domain is exposed. The Redgate Domain exclusively has protolith ages of ~1090 Ma (Fig. 10), which is unlike rocks elsewhere in the Leeuwin Complex. The predominant gneissic foliation dips shallowly with variable strike, but mainly dips in eastward directions (Fig. 7). This foliation wraps around lenses on the order of one to tens of metres long and several metres wide that contain sets of harmonic folds (of S_1) with relatively angular hinges. Fold axial surfaces and/or sheared limbs are commonly occupied by leucosomes. This has also reported at Bob's Hollow to the south of Redgate by Harris (2003), who interpreted this phenomenon as a consequence of back-rotation during shearing (Fig. 19). At the margins of the pods, these folds are rotated into parallelism with the enveloping foliation, indicating that either the wrapping fabric is relatively younger (i.e., is a composite S_1/S_2 fabric), or that strain was portioned between the fold-bearing pods and the encasing foliation during progressive deformation. Nevertheless, both fold-bearing pods and the gently dipping foliation that surrounds them are consistent with non-coaxial shearing. Lineations at Redgate (L_1?) tend to plunge down-dip of the foliation that wraps the pods (Fig. 7).

Leucosomes (and thin pegmatite dykes) at Redgate have variable relationships with the shallowly-dipping foliation, ranging from completely transposed within the foliation (Fig. 20), obliquely cross-cutting the foliation, to occupying high strain zones of small-scale shear zones that deform the foliation. Where pegmatite dykes have been transposed and recrystallised, relict porphyroclasts of feldspar give the rocks the appearance of augen gneiss. Asymmetric kinematic indicators, such as sigma and delta porphyroclasts, are rare and do not clearly show a consistent shear sense.

Bands of amphibolite within the garnet-bearing gneiss dip gently, parallel with the dominant gneissic foliation.

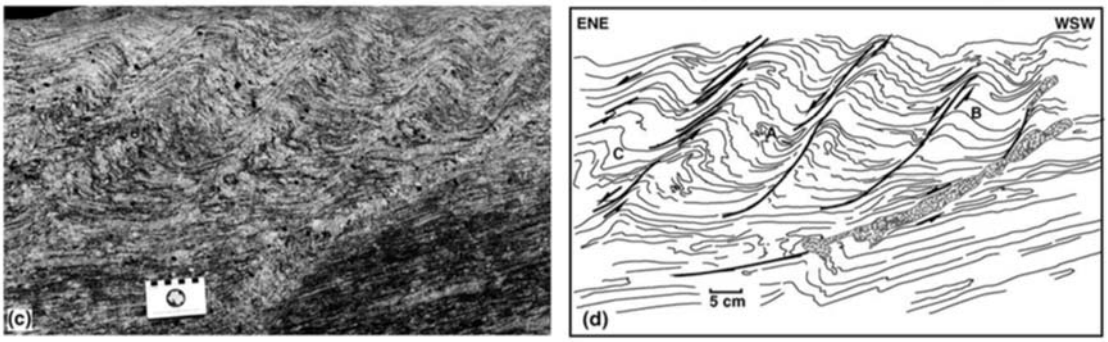

Figure 19. *Back-rotated folds between normal shear zones at Bob's Hollow to the south of Redgate Beach (after Harris, 2003).*

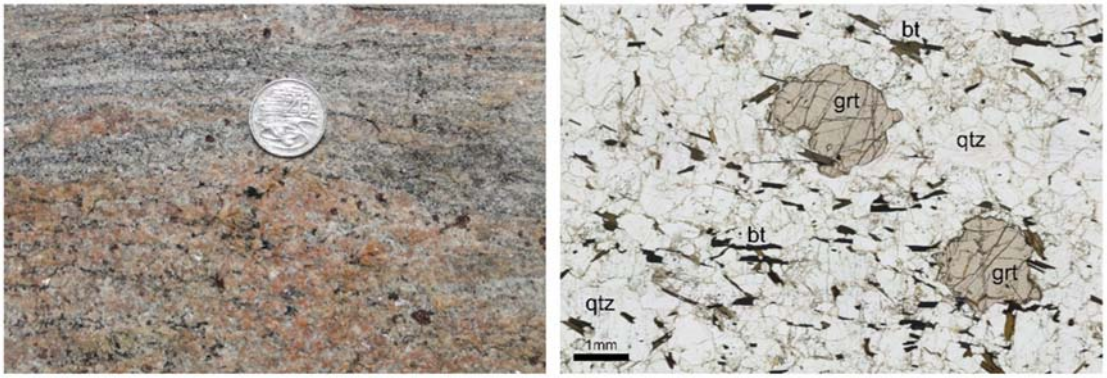

Figure 20. *Garnet-bearing orthogneiss from Redgate Beach. Sample LC08B of Arnoldi (2017). Zircon grains extracted from this sample preserve a U-Pb protolith age of 1095 ± 11 Ma, ca. 550 Ma metamorphic rims, and Hf T_{DM} age of ca. 2.2 Ga (Fig. 10).*

Points for discussion

- **Foliation timing and nomenclature** – What is the relative timing of the dominant flat-lying foliation and folded foliation to gneissic foliations elsewhere in the Leeuwin Complex? This links to a more general issue associated with of assigning numbers to foliations at individual localities (e.g., S_1, S_2) and correlating them across isolated outcrops of areas that have undergone multiple episodes of deformation.
- **Flat fabric** – What is the tectonic significance of the gently-dipping fabric and folds?
- **Metamorphic grade** – At what metamorphic conditions did the foliation(s) and folds form?

Wilyabrup Cliffs, Gracetown/Yallingup Domain, Leeuwin Complex

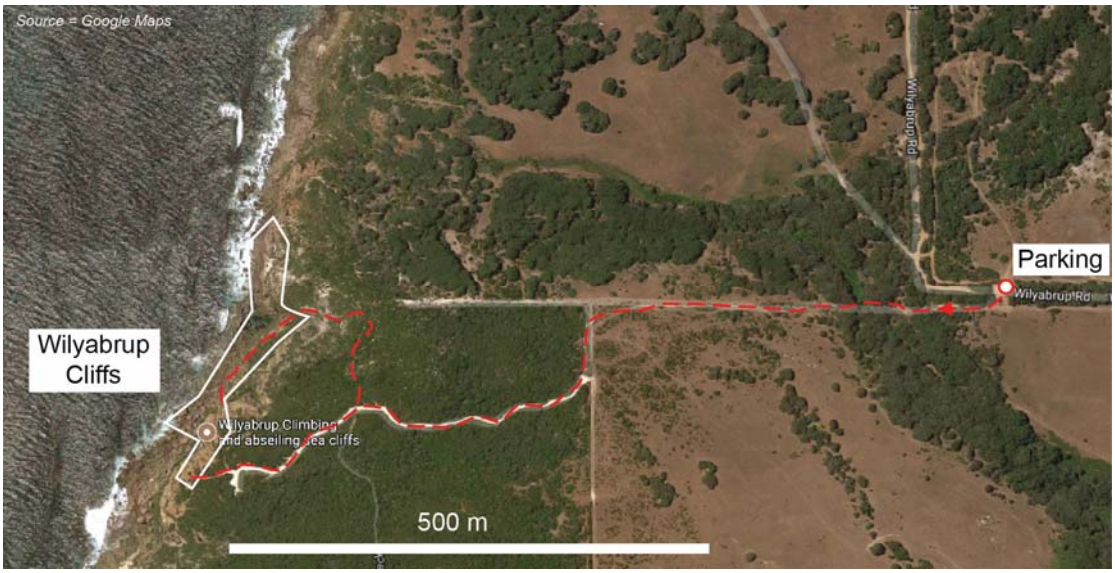

How to get there

From Caves Road, take Wilyabrup Road toward the coast. Continue for ~2.5 km to a rudimentary car parking area after two 90 bends in the road. Cross a fence on the south side of the road and take the track westward, following the signs to Wilyabrub Climbing Cliffs. Walk through a wooded valley, crossing a bridge over a small creek, and continue west. Climb over another fence and continue on the wide limestone path. A lovely view from the cliff top can be seen by continuing straight ahead. To access the base of the cliffs, take the Cape-to-Cape track north from the top of the ridge. This winds down some sturdy steps and out on to rocky outcrops of the Leeuwin Complex almost at sea level. Continue left (southwest) to the base of the cliffs, or take a right (northeast) to traverse the lower-level outcrops along the coastline to the northeast

Specific Hazards

- *Waves may surge over rocky pavements at high tide or in a significant swell.*
- *Take extra care climbing and walking over boulders.*
- *Wilyabrup is a popular rock climbing location. Be aware of people rock climbing and abseiling – keep away from their activities due to risks of falling material, and DO NOT throw rocks or anything else from the cliff tops.*

Geology

This location is close to the boundary between the Gracetown and Yallingup Domains. The rocks are dominated by felsic gneiss, which contain black amphibolite layers of variable thicknesses. The centre of a ~3m thick amphibolite layer near the base of the cliffs contains garnet porphyroblasts with coronas of hornblende and plagioclase (Fig. 21A). Garnet is absent toward the margin of this layer, where the amphibolite is strongly foliated. An amphibolite layer in this structural position can be traced along the coast to the north for several kilometres. However, garnet is only present at Wilyabrup Cliffs. The dominant gneissic foliation (S_1) is very gently dipping to the east (Fig. 7). Lineations developed on S_1 plunge down dip to E-ESE (Fig. 7). Amphibolite layers can be discontinuous, boundinaged lenses, and commonly define rootless recumbent isoclinal folds with axial planes that are parallel to S_1 (Fig. 21C-D). Leucosomes in the felsic gneiss bear large garnet porphyroblasts that comprise clusters of smaller garnet crystals Fig. 21B).

Points for discussion

- **Garnet in the amphibolite** – Does this indicate an early metamorphic event that has been overprinted elsewhere?
- **Flat fabric** – What is the tectonic significance of the sub-horizontal fabric?
- **Lineation** – Is the lineation linked to motion along the boundary between the Gracetown and Yallingup Domains?

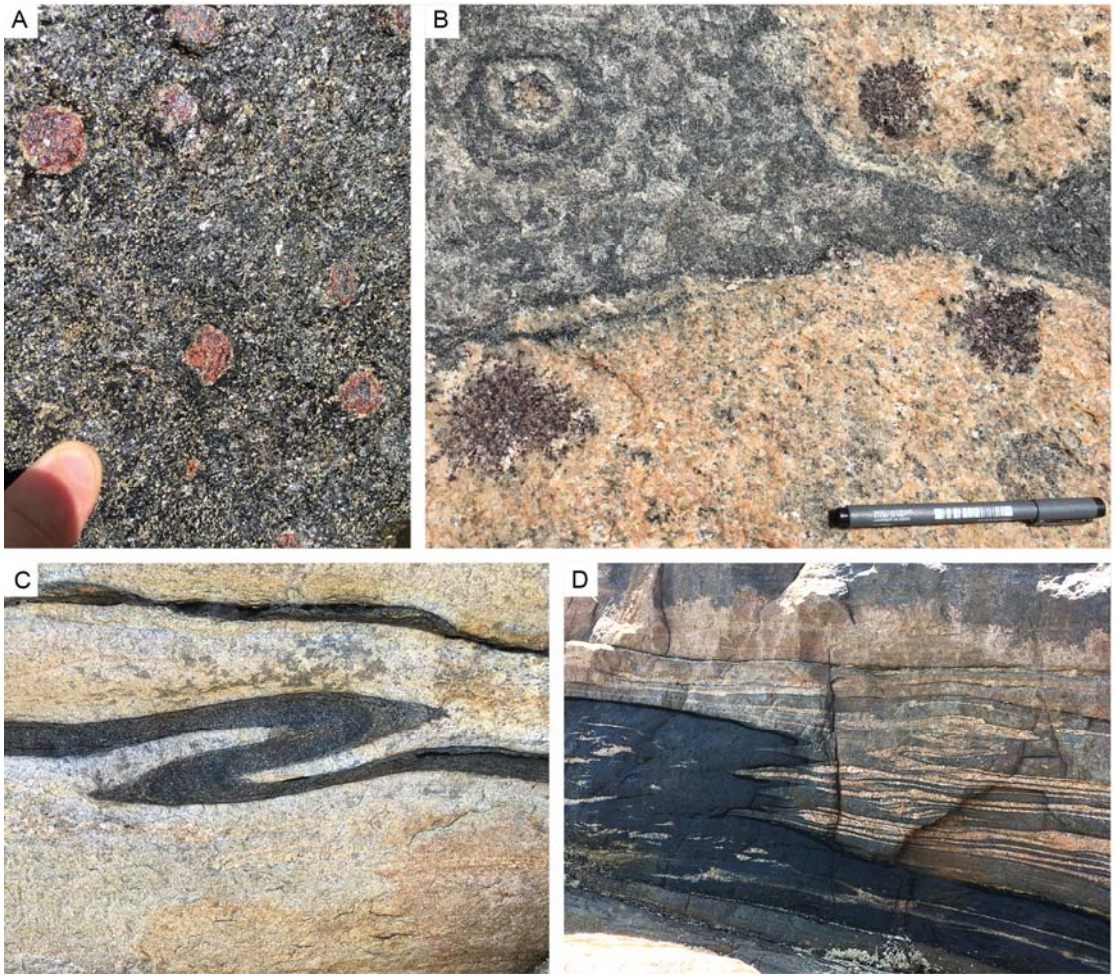

Figure 21. *A. Garnet-bearing amphibolite at Wilyabrup Cliffs, 0314785 mE, 6257863 mN. B. Garnet in leucosomes in felsic gneiss, north of Wilyabrup Cliffs. C. Recumbent isoclinal folds in amphibolite layer. North of Wilyabrup Cliffs, 0314420 mE, 6260396 mN. Isoclinal recumbent folds in felsic gneiss, leucosomes and amphibolite layer. North of Wilyabrup Cliffs, 0314420 mE, 6260400 mN.*

Canal Rocks, Smiths Point, Yallingup Domain, Leeuwin Complex

How to get there

From Caves Road, turn on to Canal Rocks Road. Continue to the huge paved carpark at the end of the road. Canal Rocks are directly next to the carpark. A walkway has been built across the gaps in the rocks for tourists.

Access to some outcrops on the east of the north-facing bay can be accessed via the boat ramps and beach.

For Smiths Point, head back along Canal Rocks Road and turn down Smiths Beach Road. Drive past the resort on your left to Smiths Point. A few modest parking places are on the north side of the road at Smiths Point.

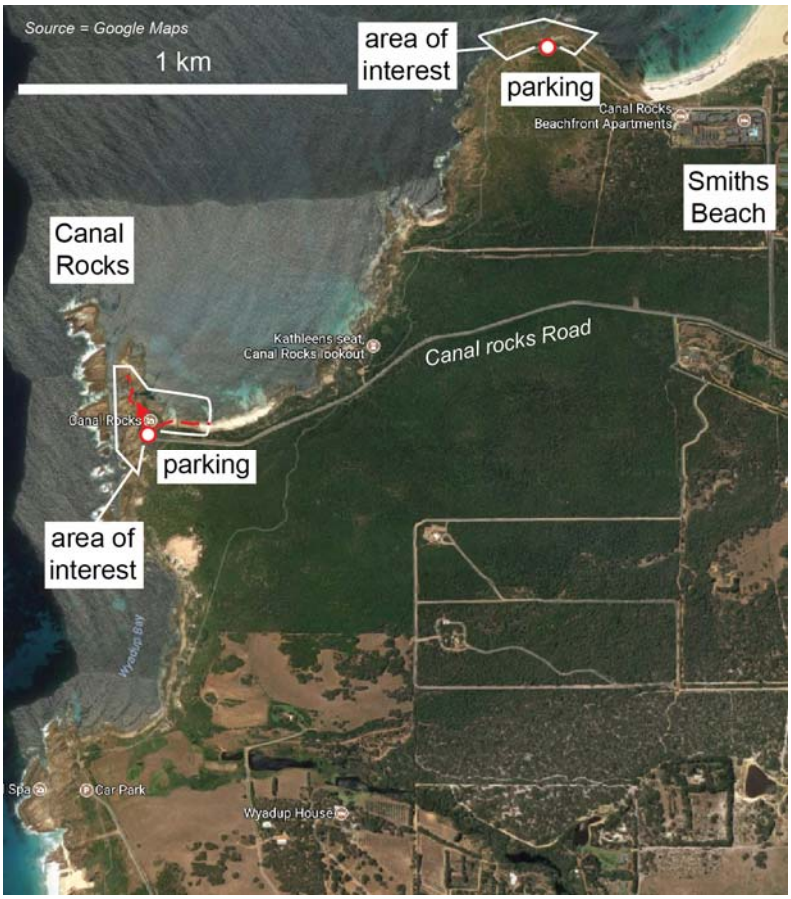

Specific Hazards

- *Waves may surge over rocky pavements at high tide or in a significant swell.*
- *Take extra care climbing and walking over boulders.*

Geology

This region is in the hinge zone of a prominent NNW-trending regional fold visible in the Yallingup Domain in aeromagnetic images. Prominent headlands of Wyadup Point, Canal Rocks and Smiths Point dominated by felsic gneiss correspond with bands of low magnetic intensity, and are separated by sandy bays that correspond with bands of high magnetic intensity on the aeromagnetic images. On the western limb, the gneissic foliation (S_1) at Wyadup and Canal Rocks dips steeply E and ENE, respectively. At Smiths point, which is near the hinge of the regional fold, S_1 dips moderately NE and NW. This geometry is consistent with a gently- to moderately N/NNE-plunging antiform, which is possibly slightly overturned to the west.

Points for discussion

- **Domain Boundary kinematics** – are these folds related to the motion on the boundaries between the Naturalite, Yallingup, and Gracetown Domains?
- **D_2 from Cape to Cape** - How does this antiform relate to the large-scale folds at Cape Leeuwin.

Sugar Loaf Rock, Yallingup Domain, Leeuwin Complex

How to get there

Head along Cape Naturaliste Road and take the turning on to Sugarloaf Road (south of Bunker Bay Road). Head to the well-paved carpark at the end. Walk up the steps to Sugarloaf Rock lookout. Veer left before you reach the top, heading down well-used a track and on to the mound-like rocky outcrop to the south of Sugarloaf Rock.

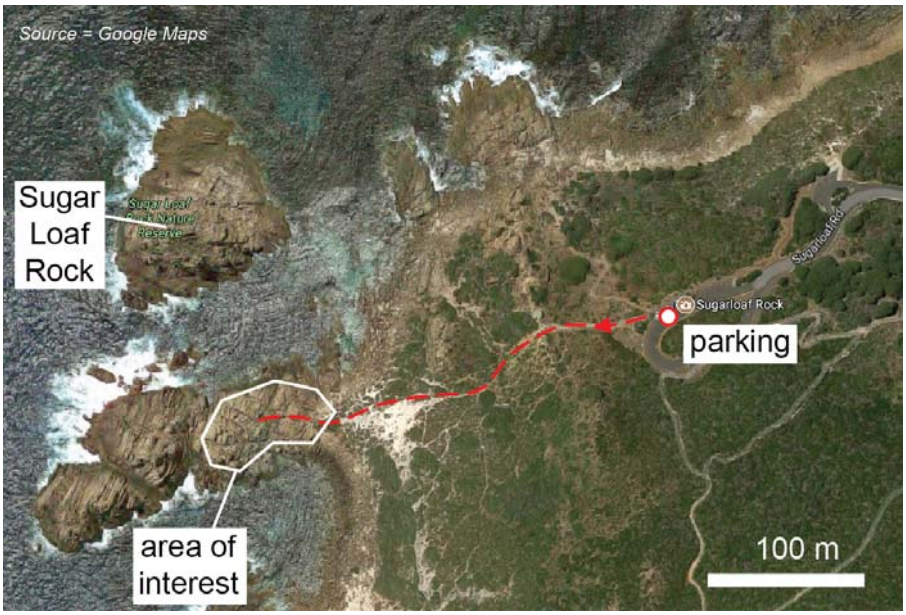

Specific Hazards

- *Waves may surge over rocky pavements at high tide or in a significant swell.*
- *Take extra care climbing and walking over boulders.*

Geology

This locality is close to the eastern margin of the Naturaliste Domain. Here, a large-scale asymmetric antiform is defined by weakly-magnetic pink felsic orthogneiss folded around a core of strongly-magnetic banded grey gneiss. Bands in the grey gneiss are on the centimetre to decimetre scale, and vary in composition from mafic to felsic, and contain distinctive boudinaged dark layers with leucosomes commonly occupying the boudin necks (Fig. 22A, B). The felsic orthogneiss is relatively homogeneous, and is interleaved with the grey gneiss at their boundary (Fig. 22C). A ~1 m wide pegmatite dyke outcrops in the core of the antiform.

The main antiform is approximately 100 m across, is moderately inclined (axial plane dips ~ESE), plunges ~30° ~NE, and is assigned to D_2 (Collins, 2003; Janssen et al., 2003). Lineations are generally parallel to the fold hinge (Fig. 7). Parasitic folds in the grey gneiss deform pre-existing boudins. Folds of similar scale and geometry to the large-scale fold can be seen on the southern face of Sugar Loaf Rock to the north. These folds have been mapped by Collins (2003) as being on the overturned western limb of the kilometre-scale Cape Naturaliste Antiform.

The asymmetry of the antiform is consistent with southwest-verging thrust-related folding.

Protoliths of pink felsic orthogneiss and banded grey gneiss at Sugar Loaf Rock were emplaced at ca. 750 Ma, and record metamorphic zircon growth at ca. 522 Ma (Collins, 2003; Janssen et al., 2003).

Points for discussion

- **Folded boudins** - What is the relationship between partial melting and deformation history?
- **Domain Boundary kinematics** – are these folds related to the motion on the boundary between the Naturalite and Yallingup Domains?
- **D_2 from Cape to Cape** - How does this antiform relate to the large-scale folds at Cape Leeuwin.
- **Metamorphism** - What metamorphic grade was achieved?

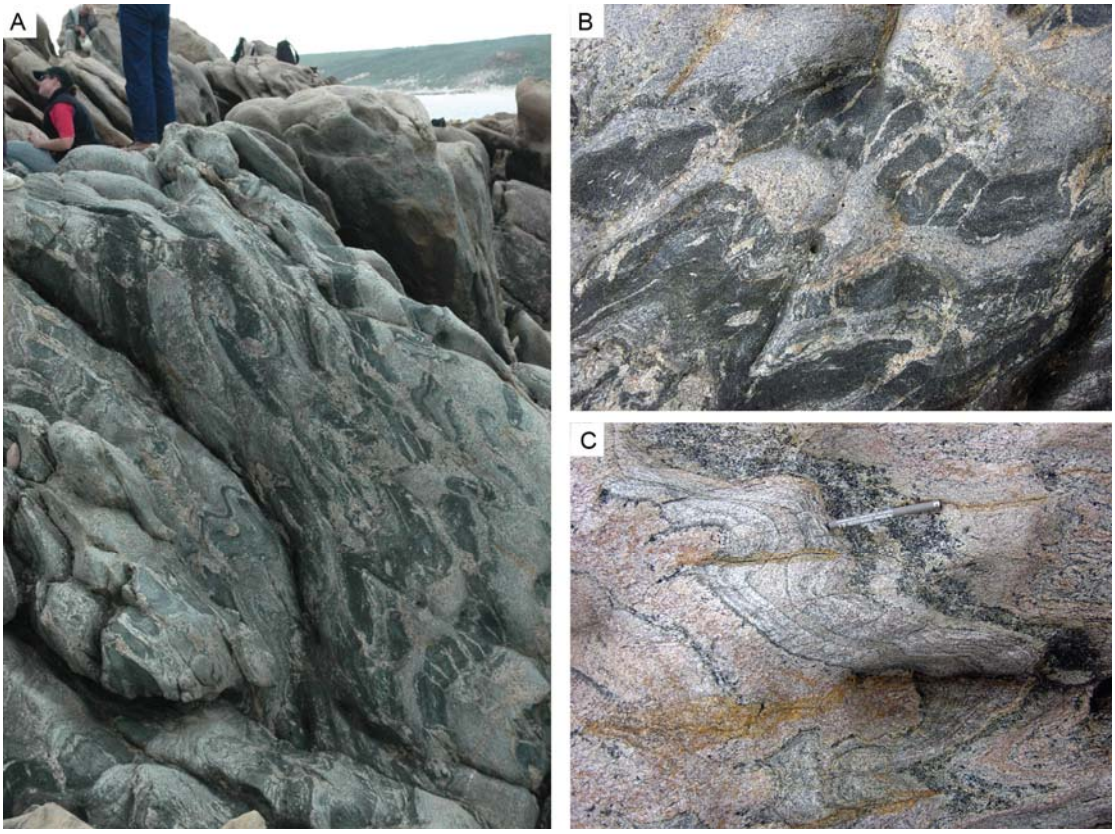

Figure 22. *A. Folded interlayered intermediate to mafic gneiss in the overturned southwestern limb of the Sugar Loaf Rock antiform, 0314857 mE, 6284774 mN. B. Folded mafic layers with pre-folding leucosomes, 0314857 mE, 6284774 mN. C. Folded interlayered gneiss of various mixed compositions, 0314857 mE, 6284774 mN. Image in A courtesy of Steven Reddy.*

Shelley Cove, Naturaliste Domain, Leeuwin Complex

How to get there

From Cape Naturaliste Road, turn of to Bunker Bay Road and continue to the multi-level loop carpark at the end. Amble down to the rocky point via the path(s).

Walk over Shelley Beach to rocky outcrops near the cliffs. Access to the rocks beneath the cliffs usually requires traversing seaweed in the northwest of the bay. The headland to the north can be accessed at low tide and small swells.

Specific Hazards

- *Waves may surge over rocky pavements at high tide or in a significant swell.*
- *Take extra care climbing and walking over boulders.*
- *Be very careful underneath the cliffs. Watch out for falling debris, and don't shelter underneath in heavy rains due to potential collapse. Don't climb the cliffs – they are unstable.*

Geology

Gneisses of the Naturaliste domain outcrop on a small headland to the east, in the centre of Shelley Cove, and to the northwest around Cape Naturaliste. On the eastern headland, granitic gneiss contains leucosomes that are variably transposed into the gneissic foliation (S_1), which dips moderately to the northwest (Fig. 7). These rocks also preserve a strong mineral lineation the plunges down-dip (Figs 7 and 23A). Joints are commonly lined with epidote and have halos of pink-stained feldspar (Fig. 23B).

A steeply dipping, SE-trending small-scale shear zone displaces garnet-bearing felsic gneiss in the centre of the Cove (Fig. 23C). Garnet has been retrogressed to chlorite in the shear zone, and smeared chlorite clots (after garnet) define a steeply plunging lineation in the high strain part of the shear zone. This shear zone can also be seen in the weathered cliff section to the northwest. To its northeast along the cliff section, a granitic dyke has intruded a mafic gneiss/granulite with abundant leucosomes. Zircon from this mafic unit yield a U–Pb age of 536 ± 21 Ma (Simons, 2001), which has been interpreted by Janssen et al. (2003) as a high grade metamorphic event that resulted in generation of the leucosomes.

On the northwest side of Shelly Cove, the Leeuwin Complex is unconformably overlain by the Quaternary Tamala Limestone (Fig. 23C). A basal conglomerate is deposited directly above the unconformity, and has boulder-sized clasts of gneisses that are common in the Leeuwin Complex. The top of this unit is strongly planar, and is overlain by a dune a cross-bedded facies that forms the high cliffs.

Points for discussion

- **Lineation** – What is the tectonic significance of the strong lineation in the L-S tectonite?
- **Epidote-bearing joints** – When did they form, and at what conditions? What is the significance of epidote-bearing fractures?

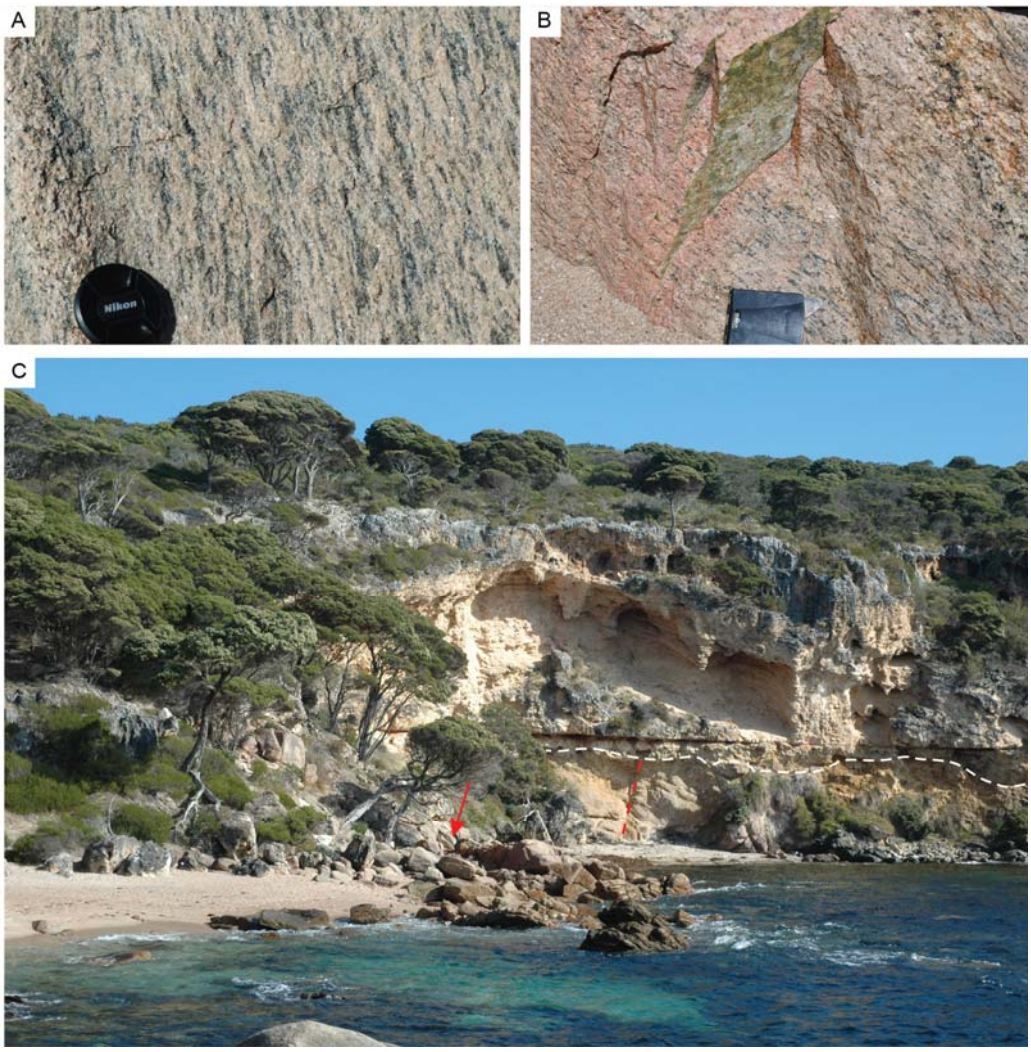

Figure 23. *Field photos from Shelley Cove. A. Felsic with a strong lineation. B. Epidote-bearing joint in felsic gneiss with pink halo of oxidized feldspar. C. Tamala Limestone unconformably overlaying the Leeuwin Complex, viewing northwest. Unconformity indicated by white dashed line. Dune cross-bedded facies forms the main cliff section. Red dashed line indicates a small steeply-dipping shear zone in the weathered Leeuwin Complex. In a fresh outcrop of the shear zone (red arrow), garnet in the host rock is retrogressed in the high strain domain, defining a lineation.*

Bunbury Basalt, Casuarina Point, Bunbury, Perth Basin

How to get there

Drive through Bunbury along Ocean Drive. North of the roundabout of Symmons Street and Ocean Drive, turn into a large carpark at 'Wyalup Rocky Point' opposite Bunbury Recreation Oval. Walk down the stepped track to the rocky outcrops on the coast.

Specific Hazards

- *Waves may surge over rocky pavements at high tide or in a significant swell.*
- *Take extra care climbing and walking over boulders.*

Geology

A basaltic lava flow of the Bunbury Basalt is exposed along the shoreline from this location to Casuarina Point to the north, collectively known as the Casuarina Point locality. Columnar joints are well-developed but quite irregular (Fig. 24). The basalt is plagioclase porphyritic, with phenocrysts up to 10 mm long (Fig. 25).

This particular outcrop is located along the western margin of the Bunbury Paleovalley, which confined the lava flows. The Bunbury Paleovalley meandered along the axis of the N-S trending Bunbury Trough, and the geometry of its tributaries indicate south-to-north drainage (Olierook et al., 2015b) (Fig. 13). The Bunbury Basalt also erupted into another, older paleovalley – the Donnybrook Paleovalley – also drained axially but was located proximal to the Darling Fault to the east (Fig. 13).

The thickness of basalt at Casuarina Point is approximately 20 m, but typically reaches ~70 m thick in centre of the paleovalley elsewhere, and to over 200 m in the vicinity of Black Point along the southern coast (Fig. 13). The Bunbury Basalt was erupted in three phases – the first at 136.96 ± 0.43 Ma in the Donnybrook Paleovalley, which coincides with the switch from rift to drift. This is followed by two pulses at 132.71 ± 0.43 and 130.45 ± 0.82 Ma in the Bunbury Paleovalley, which are separated by thin sediments (Olierook et al., 2016).

Points for discussion

- **Pathway and eruption** – Where/what was the site of eruption for the Bunbury Basalt?
- **Unique** – Why is the Bunbury Basalt the only volcanic unit present in the Perth Basin, and why is it located in the southern Perth Basin?
- **Source** – Was the relative contributions of the Kerguelen plume versus passive rift-related decompression on the generation of Bunbury Basalt melts?

- **Drainage in the Perth Basin** – Why has the drainage in the Perth Basin changed from S-N pre-breakup to E-W post-breakup?

Figure 24. *Columnar jointed basalt at Rocky Point.*

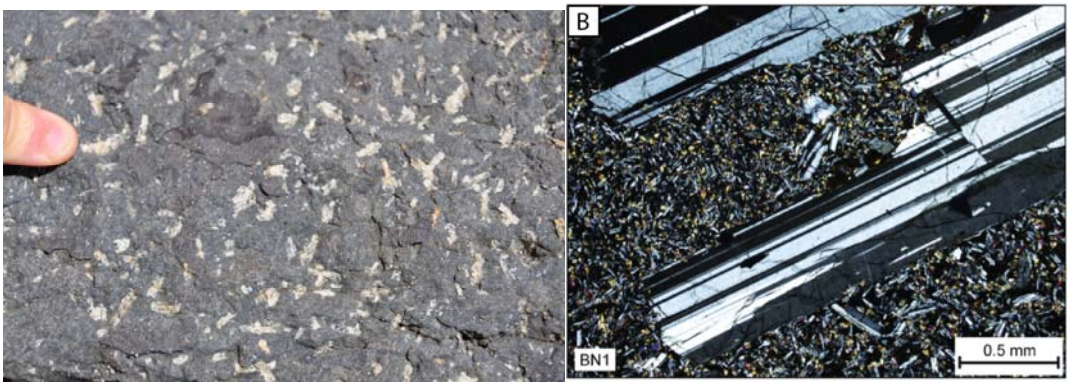

Figure 25. *A. Porphyritic basalt at Rocky Point. B. Photomicrograph of basalt from Rocky Point. Cross polarized light. After Olierook et al. (2016).*

References

Aitken, A.R.A., Betts, P.G., Young, D.A., Blankenship, D.D., Roberts, J.L., Siegert, M.J., 2016. The Australo-Antarctic Columbia to Gondwana transition. Gondwana Research 29, 136-152.

Arnoldi, S., 2017. Spatial and temporal relationships in rocks of the Leeuwin Complex, and their setting within the Pinjarra Orogen of Western Australia, Department of Applied Geology. Curtin University, BSc (Hons) Thesis, Unpublished.

Arnoldi, S., Fitzsimons, I.C.W., Timms, N.E., 2017. Spatial and temporal relationships in rocks of the Leeuwin Complex, and their setting within the Pinjarra Orogen of Western Australia, in: Pearce, M.A. (Ed.), SGTSG Denmark 2017 abstract volume: Biennial meeting of the Specialist Group in Tectonics and Structural Geology, Geological Society of Australia, 8--12 November 2017, Denmark, Western Australia. Geological Survey of Western Australia, Denmark, Western Australia, p. 32.

Barnett-Moore, N., Flament, N., Heine, C., Butterworth, N., Müller, R.D., 2014. Cenozoic uplift of south Western Australia as constrained by river profiles. Tectonophysics 622, 186-197.

Beeson, J., Harris, L.B., Delor, C.P., 1995. Structure of the western Albany Mobile Belt (southwestern Australia): evidence for overprinting by Neoproterozoic shear zones of the Darling Mobile Belt. Precambrian Research 75, 47-63.

Black, L.P., Harris, L.B., Delor, C.P., 1992. Reworking of Archaean and early Proterozoic components during a progressive, middle Proterozoic tectonothermal event in the Albany Mobile Belt, Western Australia. Precambrian Research 59, 95-123.

Bodorkos, S., Fitzsimons, I., Hall, L., Sircombe, K., Lewis, C., 2016. Beneath the Perth Basin: new U-Pb SHRIMP zircon ages from the Pinjarra Orogen, Western Australia, 2016. Geoscience Australia Record 2016/13.

Boger, S.D., 2011. Antarctica — Before and after Gondwana. Gondwana Research 19, 335-371.

Borissova, I., 2002. Geological framework of the Naturaliste Plateau. Geoscience Australia Record 2002/20.

Bruguier, O., Bosch, D., Pidgeon, R.T., Byrne, D.I., Harris, L.B., 1999. U-Pb chronology of the Northampton Complex, Western Australia–evidence for Grenvillian sedimentation, metamorphism and deformation and geodynamic implications. Contributions to Mineralogy and Petrology 136, 258-272.

Cobb, M.M., Cawood, P.A., Kinny, P.D., Fitzsimons, I.C.W., 2001. SHRIMP U-Pb zircon ages from the Mullingarra Complex, Western Australia: Isotopic evidence for allochthonous blocks in the Pinjarra orogen and implications for East Gondwana assembly. Geological Society of Australia Abstracts 64, 21-22.

Cockbain, A.E., 1990. Perth Basin. Geology and Mineral Resources of Western Australia, Western Australia Geological Survey Memoir 3, 495-524.

Coffin, M.F., Pringle, M.S., Duncan, R.A., Gladczenko, T.P., Storey, M., Müller, R.D., Gahagan, L.A., 2002. Kerguelen hotspot magma output since 130 Ma. Journal of Petrology 43, 1121-1137.

Collins, A.S., 2003. Structure and age of the northern Leeuwin Complex, Western Australia: constraints from field mapping and U–Pb isotopic analysis. Australian Journal of Earth Sciences 50, 585-599.

Collins, A.S., Fitzsimons, I.C.W., 2001. Structural, isotopic and geochemical constraints on the evolution of the Leeuwin Complex, southwest Australia. In Geological Society of Australia Abstracts, Rodinia Symposium. Geological Soceity of Australia, Perth, pp. 16-19.

Compston, W., Williams, I.S., McCulloch, M.T., 1986. Contrasting zircon U‐Pb and model Sm‐Nd ages for the Archaean Logue Brook Granite. Australian Journal of Earth Sciences 33, 193-200.

Crostella, A., Backhouse, J., 2000. Geology and petroleum exploration of the central and southern Perth Basin, Western Australia. Geological Society of Western Australia Report 57, 85p.

Czarnota, K., Hoggard, M.J., White, N., Winterbourne, J., 2013. Spatial and temporal patterns of Cenozoic dynamic topography around Australia. Geochemistry, Geophysics, Geosystems 14, 634-658.

Dentith, M.C., Bruner, I., Long, A., Middleton, M.F., Scott, J., 1993. Structure of the eastern margin of the Perth Basin, Western Australia. Exploration Geophysics 24, 455-462.

Direen, N.G., 2011. Comment on “Antarctica — Before and after Gondwana” by S.D. Boger Gondwana Research, Volume 19, Issue 2, March 2011, Pages 335–371. Gondwana Research 21, 302-304.

Embleton, B.J.J., Schmidt, P.W., 2007. Age and significance of magnetizations in dolerite dykes from the Northampton Block, Western Australia. Australian Journal of Earth Sciences 32, 279-286.

Evans, T., 1999. Extent and nature of the 1200 Ma Wheatbelt Dyke Swarm, South- western Australia. University of Western Australia, Unpublished.

Fitzsimons, I.C.W., 2003. Proterozoic basement provinces of southern and southwestern Australia, and their correlation with Antarctica. Geological Society, London, Special Publications 206, 93-130.

Fletcher, I.R., Libby, W.G., 1993. Further isotopic evidence for the existence of two distinct terranes in the southern Pinjarra Orogen, Western Australia. Geological Survey of Western Australia Report 37, 81-83.

Fletcher, I.R., Wilde, S.A., Rosman, K.J.R., 1985. Sm‐Nd model ages across the margins of the Archaean Yilgarn Block, Western Australia — III. The western margin. Australian Journal of Earth Sciences 32, 73-82.

Freeman, M.J., Donaldson, M.J., 2006. Geology of the southern Perth Basin and Margaret River wine district, sothwestern Western Australia - a field guide. Geological Society of Western Australia Record 2006/20.

Freeman, M.J., Donaldson, M.J., 2008. Mines and wines of southwestern Western Australia - a field guide. Geological Survey of Western Australia Record 2008/10.

Frey, F.A., McNaughton, N.J., Nelson, D.R., Duncan, R.A., 1996. Petrogenesis of the Bunbury Basalt, Western Australia: interaction between the Kerguelen plume and Gondwana lithosphere? Earth and Planetary Science Letters 144, 163-183.

Gardner, R.L., Daczko, N.R., Halpin, J.A., Whittaker, J.M., 2015. Discovery of a microcontinent (Gulden Draak Knoll) offshore Western Australia: Implications for East Gondwana reconstructions. Gondwana Research 28, 1019-1031.

Gibbons, A.D., Barckhausen, U., van den Bogaard, P., Hoernle, K., Werner, R., Whittaker, J.M., Müller, R.D., 2012. Constraining the Jurassic extent of Greater India: Tectonic evolution of the West Australian margin. Geochemistry Geophysics Geosystems 13.

Halpin, J.A., Crawford, A.J., Direen, N.G., Coffin, M.F., Forbes, C.J., Borissova, I., 2008. Naturaliste Plateau, offshore Western Australia: A submarine window into Gondwana assembly and breakup. Geology 36, 807.

Harris, L.B., 1994a. Neoproterozoic sinistral displacement along the Darling mobile belt, Western Australia, during Gondwanaland assembly. Journal of the Geological Society 151, 901-904.

Harris, L.B., 1994b. Structural and tectonic synthesis for the Perth Basin, Western Australia. Journal of Petroleum Geology 17, 129-156.

Harris, L.B., 2003. Folding in high-grade rocks due to back-rotation between shear zones. Journal of Structural Geology 25, 223-240.

Harris, L.B., Li, Z.X., 1995. Palaeomagnetic dating and tectonic significance of dolerite intrusions in the Albany Mobile Belt, Western Australia. Earth and Planetary Science Letters 131, 143-164.

Iasky, R.P., 1993. A structural study of the southern Perth Basin, Western Australia. Geological Survey of Western Australia Report 31.

Iasky, R.P., Lockwood, A.M., 2004. Gravity and magnetic interpretation of the southern Perth Basin, Western Australia. Geological Society of Western Australia Record 2004/8.

Janssen, D., Collins, A., Fitzsimons, I., 2003. Structure and tectonics of the Leeuwin Complex and Darling fault zone southern Pinjarra Orogen Western Australia - A field guide. Geological Survey of Western Australia Record 2003/15.

Janssen, D.P., 2001. SHRIMP data from the Leeuwin Complex.

Jones, A.T., Kelman, A.P., Kennard, J.M., Le Poidevin, S., Mantle, D.J., Mory, A.J., 2012. Offshore Perth Basin biozonation and stratigraphy 2011, chart 38. Geoscience Australia.

Ksienzyk, A.K., Jacobs, J., Boger, S.D., Košler, J., Sircombe, K.N., Whitehouse, M.J., 2012. U–Pb ages of metamorphic monazite and detrital zircon from the Northampton Complex: evidence of two orogenic cycles in Western Australia. Precambrian Research 198-199, 37-50.

Libby, W.G., de Laeter, J.R., 1998. Biotite Rb‐Sr age evidence for Early Palaeozoic tectonism along the cratonic margin in southwestern Australia∗. Australian Journal of Earth Sciences 45, 623-632.

Lu, S., Phillips, D., Kohn, B.P., Gleadow, A.J.W., Matchan, E.L., 2015. Thermotectonic evolution of the western margin of the Yilgarn craton, Western Australia: New insights from 40 Ar/ 39 Ar analysis of muscovite and biotite. Precambrian Research 270, 139-154.

Markwitz, V., Kirkland, C.L., Evans, N.J., 2017. Early Cambrian metamorphic zircon in the northern Pinjarra Orogen: Implications for the

structure of the West Australian Craton margin. Lithosphere 9, 3-13.

McCulloch, M.T., 1987. Sm‐Nd isotopic constraints on the evolution of Precambrian crust in the Australian continent. Proterozic Lithospheric Evolution, 115-130.

Morrissey, L.J., Payne, J.L., Hand, M., Clark, C., Taylor, R., Kirkland, C.L., Kylander-Clark, A., 2017. Linking the Windmill Islands, east Antarctica and the Albany–Fraser Orogen: Insights from U–Pb zircon geochronology and Hf isotopes. Precambrian Research 293, 131-149.

Mory, A.J., Iasky, R.P., 1996. Stratigraphy and structure of the onshore northern Perth Basin, Western Australia. Geological Survey of Western Australia Report 46.

Murphy, D.M.K., 1992. The geology of the Leeuwin Block, Western Australia: Perth, Western Australia, Department of Applied Geology. Curtin University of Technology, Unpublished, p. 164p.

Myers, J.S., 1990a. Albany–Fraser Orogen. Geological Survey of Western Australia Memoir v. 3, 255-263.

Myers, J.S., 1990b. Geological note: Anorthosite in the Leeuwin Complex of the Pinjarra Orogen, Western Australia. Australian Journal of Earth Sciences 37, 241-245.

Myers, J.S., 1990c. Pinjarra Orogen. Geological Survey of Western Australia Memoir v. 3, 264-274.

Myers, J.S., 1994. Late Proterozoic High-grade Gneiss Complex Between Cape Leeuwin and Cape Naturaliste: Excursion Guidebook 6. Geological Society of Australia (WA Division).

Myers, J.S., Shaw, R.D., Tyler, I.M., 1996. Tectonic evolution of Proterozoic Australia. Tectonics 15, 1431-1446.

Nelson, D.R., 1995. Field guide to the Leeuwin Complex, Australian Conference on Geochronology and Isotope Geoscience. Geological Survey of Western Australia Perth, p. 24p.

Nelson, D.R., 1996. Compilation of SHRIMP U–Pb zircon geochronology data, 1995. Western Australian Geological Survey Record 1996/5, 168.

Nelson, D.R., 1999. Compilation of SHRIMP U–Pb zircon geochronology data, 1998. Western Australia Geological Survey Record 1999/2, 222.

Nelson, D.R., 2002. Compilation of geochronological data, 2001: Western Australia Geological Survey. Western Australia Geological Survey Record 2002/2, 282.

Nemchin, A.A., Pidgeon, R.T., 1998. Precise conventional and SHRIMP baddeleyite U‐Pb age for the Binneringie Dyke, near Narrogin, Western Australia. Australian Journal of Earth Sciences 45, 673-675.

Nemchin, A.A., Pidgeon, R.T., 1999. U–Pb ages on titanite and apatite from the Darling Range granite: implications for Late Archaean history of the southwestern Yilgarn Craton. Precambrian Research 96, 125-139.

Norvick, M.S., Smith, M.A., Power, M.R., 2001. The plate tectonic evolution of eastern Australasia guided by the stratigraphy of the Gippsland Basin, in: Hill, K.C., Bernecker, T. (Eds.), Eastern Australasian Basins Symposium 2001. Petroleum Exploration

Society of Australia Special Publication, pp. 15-23.

Olierook, H.K.H., Jourdan, F., Merle, R.E., Timms, N.E., Kusznir, N., Muhling, J.R., 2016. Bunbury Basalt: Gondwana breakup products or earliest vestiges of the Kerguelen mantle plume? Earth and Planetary Science Letters 440, 20-32.

Olierook, H.K.H., Merle, R.E., Jourdan, F., Sircombe, K., Fraser, G., Timms, N.E., Nelson, G., Dadd, K.A., Kellerson, L., Borissova, I., 2015a. Age and geochemistry of magmatism on the oceanic Wallaby Plateau and implications for the opening of the Indian Ocean. Geology 43, 971-974.

Olierook, H.K.H., Timms, N.E., 2016. Quantifying multiple Permian-Recent exhumation events during the break-up of eastern Gondwana: sonic transit time analysis of the central and southern Perth Basin. Basin Research 28, 796-826.

Olierook, H.K.H., Timms, N.E., Merle, R.E., Jourdan, F., Wilkes, P.G., 2015b. Paleodrainage and fault development in the southern Perth Basin, Western Australia during and after the breakup of Gondwana from 3D modelling of the Bunbury Basalt. Australian Journal of Earth Sciences, 1-17.

Olierook, H.K.H., Timms, N.E., Wellmann, J.F., Corbel, S., Wilkes, P.G., 2015c. 3D structural and stratigraphic model of the Perth Basin, Western Australia: Implications for sub-basin evolution. Australian Journal of Earth Sciences 62, 447-467.

Partington, G.A., McNaughton, N.J., Williams, I.S., 1995. A review of the geology, mineralization, and geochronology of the Greenbushes Pegmatite, Western Australia. Economic Geology 90, 616-635.

Pearce, D.J., 2014. Re-evaluating the structure and tectonic development of the Northern Leeuwin Complex: constraints from aeromagnetic and gravity data, Dpeartment fo Applied Geology. Curtin University, BSc (Honours) Thesis, Unpublished.

Pearce, J.A., Harris, N.B., Tindle, A.G., 1984. Trace element discrimination diagrams for the tectonic interpretation of granitic rocks. Journal of petrology 25, 956-983.

Pidgeon, R.T., Cook, T.J.F., 2003. 1214±5 Ma dyke from the Darling Range, southwestern Yilgarn Craton, Western Australia. Australian Journal of Earth Sciences 50, 769-773.

Pidgeon, R.T., Nemchin, A.A., 2001. 1.2 Ga Mafic dyke near York, southwestern Yilgarn Craton, Western Australia. Australian Journal of Earth Sciences 48, 751-755.

Pisarevsky, S.A., Wingate, M.T.D., Li, Z.-X., Wang, X.-C., Tohver, E., Kirkland, C.L., 2014. Age and paleomagnetism of the 1210Ma Gnowangerup–Fraser dyke swarm, Western Australia, and implications for late Mesoproterozoic paleogeography. Precambrian Research 246, 1-15.

Playford, P.E., Low, G.H., Cockbain, A.E., 1976. Geology of the Perth Basin, Western Australia. Geological Survey of Western Australia, 124 pp.

Qiu, Y., McNaughton, N.J., Groves, D.I., Dunphy, J.M., 1999. First record of 1.2 Ga quartz dioritic magmatism in the Archaean Yilgarn Craton, Western Australia, and its significance. Australian Journal of Earth Sciences 46, 421-428.

Rasmussen, B., Fletcher, I.R., 2004. Zirconolite: A new U-Pb chronometer for mafic igneous rocks. Geology 32, 785-788.

Sayers, J., Symonds, P.A., Direen, N.G., Bernardel, G., 2001. Nature of the continent-ocean transition on the non-volcanic rifted margin of the central Great Australian Bight. Geological Society, London, Special Publications 187, 51-76.

Simons, S.L., 2001. Nature and origin of the mafic dykes within the late Proterozoic Leeuwin Complex, Western Australia: Perth, Western Australia, Department of Applied Geology. Curtin University of Technology, BSc (Honours) Thesis, Unpublished.

Song, T., Cawood, P.A., 2000. Structural styles in the Perth Basin associated with the Mesozoic break-up of Greater India and Australia. Tectonophysics 317, 55-72.

Spaggiari, C., Kirkland, C., Pawley, M., Smithies, R., Wingate, M., Doyle, M., Blenkinsop, T., Clark, C., Oorschot, C., Fox, L., Savage, J., 2011. The geology of the east Albany–Fraser Orogen — a field guide. Geological Survey of Western Australia Record 2011/23, 97p.

Spaggiari, C., Kirkland, C., Smithies, R., Occhipinti, S.A., Wingates, M., 2014. Geological framework of the Albany-Fraser Orogen, in: Spaggiari, C., Tyler, I.M. (Eds.), Albany-Fraser Orogen Seismic and Magnetotelluric (MT) Workshop 2014: Extended Abstracts. Geological Survey of Western Australia, Record 2014/06, pp. 12-27.

Stoltze, A., 2000. Structural and metamorphic investigation of part of the northern Leeuwin Complex: Perth, Western Australia, Department fo Applied Geology. Curtin University, BSc (Honours) Thesis, Unpublished.

Teasdale, J.P., Pryer, L.L., Stuart-Smith, P.G., Romine, K.K., Etheridge, M.A., Loutit, T.S., Kyan, D.M., 2003. Structural framework and basin evolution of Australia's southern margin. The APPEA Journal 43, 13-47.

Timms, N.E., 2017. Mid-conference Field Trip Guide: The Western Nornalup Zone, Albany-Fraser Orogen, Western Australia.

Timms, N.E., 2018. SGTSG post-conference field trip guide: the Leeuwin Complex, Western Australia. Geological Survey of Western Australia, Perth, p. 40p.

Totterdell, J.M., Blevin, J.E., Struckmeyer, H.I.M., Bradshaw, B.E., Colwell, J.B., Kennard, J.M., 2000. Anew sequence framework for the Great Australian Bight: Starting with a clean slate. The APPEA Journal 40, 95-118.

Totterdell, J.M., Bradshaw, B.E., 2004. The structural framework and tectonic evolution of the Bight Basin, in: Boult, P.J., Johns, D.R., Lang, S.C. (Eds.), PESA's Eastern Australian Basins Symposium II. Conference Proceedings. Petroleum Exploration Society of Australia, Special Publication, Adelaide, South Australia, pp. 41-61.

Tucker, C., 2014. Re-evaluation of the Structural Evolution Southern Leeuwin Complex, Western Australia, Department fo Applied Geology. Curtin University, BSc (Honours) Thesis, Unpublished.

Tucker, N.M., Payne, J.L., Clark, C., Hand, M., Taylor, R.J.M., Kylander-Clark, A.R.C., Martin, L., 2017. Proterozoic reworking of Archean (Yilgarn) basement in the Bunger Hills, East Antarctica. Precambrian Research 298, 16-38.

Veevers, J.J., Powell, C.M., Roots, S.R., 2007. Review of seafloor spreading around Australia. I. synthesis of the patterns of spreading. Australian Journal of Earth Sciences 38, 373-389.

White, L.T., Gibson, G.M., Lister, G.S., 2013. A reassessment of paleogeographic reconstructions of eastern Gondwana: Bringing geology back into the equation. Gondwana Research 24, 984-998.

Wilde, S.A., 1999. Evolution of the Western Margin of Australia during the Rodinian and Gondwanan Supercontinent Cycles. Gondwana Research 2, 481-499.

Wilde, S.A., Murphy, D.M.K., 1990. The nature and origin of Late Proterozoic high-grade gneisses of the Leeuwin Block, Western Australia. Precambrian Research 47, 251-270.

Wilde, S.A., Nelson, D.R., 2001. Geology of the western Yilgarn Craton and Leeuwin Complex, Western Australia - a field guide. Geological Survey of Western Australia Record 2001/15, 41p.

Willcox, J.B., Stagg, H.M.J., 1990. Australia's southern margin: a product of oblique extension. Tectonophysics 173, 269-281.

Williams, S.E., Whittaker, J.M., Granot, R., Müller, D.R., 2013. Early India–Australia spreading history revealed by newly detected Mesozoic magnetic anomalies in the Perth Abyssal Plain. Journal of Geophysical Research, Solid Earth 118, 3275–3284.

Williams, S.E., Whittaker, J.M., Müller, R.D., 2011. Full-fit, palinspastic reconstruction of the conjugate Australian-Antarctic margins. Tectonics 30, n/a-n/a.

Wingate, M.T., Giddings, J.W., 2000. Age and palaeomagnetism of the Mundine Well dyke swarm, Western Australia: implications for an Australia–Laurentia connection at 755 Ma. Precambrian Research 100, 335-357.

Wingate, M.T.D., Campbell, I.H., Harris, L.B., 2000. SHRIMP baddeleyite age for the Fraser dyke swarm, southeast Yilgarn Craton, Western Australia. Australian Journal of Earth Sciences 47, 309-313.

Wingate, M.T.D., Kirkland, C.L., 2011. 185931: Quartz Diorite Dyke, Top Camp Well; Geochronology Record 974. Geological Survey of Western Australia, 5.

Notes and Doodles

THE INSTITUTE FOR
GEOSCIENCE RESEARCH (TIGeR)

Make tomorrow better.

Curtin University